Review

Development of Atom-Economical Catalytic Asymmetric Reactions under Proton Transfer Conditions: Construction of Tetrasubstituted Stereogenic Centers and Their Application to Therapeutics

Naoya KUMAGAI†

The University of Tokyo; 7–3–1 Hongo, Bunkyo-ku, Tokyo 113–0033, Japan.

Received October 5, 2010

The development of atom-economical catalytic asymmetric reactions based on two distinct sets of catalyst, a rare earth metal/amide-based ligand catalyst and a soft Lewis acid/hard Brønsted base catalyst, is reviewed. These catalytic systems exhibit high catalytic activity and stereoselectivity by harnessing a cooperative catalysis through hydrogen bond/metal coordination and soft–soft interactions/hard–hard interactions, respectively. The effectiveness of these cooperative catalysts is clearly delineated by the high stereoselectivity in reactions with highly coordinative substrates, and the specific activation of otherwise low-reactive pronucleophiles under proton transfer conditions. The rare earth metal/amide-based ligand catalyst was successfully applied to catalytic asymmetric aminations, nitroaldol (Henry) reactions, Mannich-type reactions, and conjugate addition reactions, generating stereogenic tetrasubstituted centers. Catalytic asymmetric amination and *anti*-selective catalytic asymmetric nitroaldol reactions were successfully applied to the efficient enantioselective synthesis of therapeutic candidates, such as AS-3201 and the β_3-adrenoreceptor agonist, showcasing the practical utility of the present protocols. The soft Lewis acid/hard Brønsted base cooperative catalyst was specifically developed for the chemoselective activation of soft Lewis basic allylic cyanides and thioamides, which are otherwise low-reactive pronucleophiles. The cooperative action of the catalyst allowed for efficient catalytic generation of active carbon nucleophiles *in situ*, which were integrated into subsequent enantioselective additions to carbonyl-type electrophiles.

Key words rare earth metal; asymmetric catalysis; atom economy; proton transfer; tetrasubstituted stereogenic center

Introduction

Asymmetric catalysis is firmly established in an unwavering position for producing enantiomerically enriched compounds with maximum efficiency.[1—3] Catalytic asymmetric processes provide a more economical and environmentally benign methodology than those using stoichiometric amounts of chiral reagents. In most cases of the production of a given chemical entity, the reaction of interest is a bimolecular reaction. The design of conventional asymmetric catalysts has largely focused on the principle of a simple Lewis acid or Lewis base activation of one of the reaction partners. Numerous asymmetric catalysts have been developed based on this strategy, and currently, most reactions can be rendered in an asymmetric manner. In this context, the central interest in this field has shifted to high activity, selectivity, and broad substrate generality under mild and environmentally benign reaction conditions. Our particular focus has been directed to the development of a cooperative catalytic system, where both reaction partners are simultaneously activated by finely tuned asymmetric catalysts. Compared with conventional catalysts, cooperative catalysts usually exhibit an enhanced catalytic activity and a higher level of stereodifferentiation under mild reaction conditions, thereby attracting much attention as the next-generation catalysts for prospective practical applications.[4—11] Nature harnesses the power of bifunctional catalysis in a number of vital enzymatic reactions, showing the effectiveness of such a strategy for chemical transformations under remarkably mild conditions.

In this review, two distinct sets of catalyst, a rare earth (RE) metal/amide-based ligand catalyst and a soft Lewis acid/hard Brønsted base catalyst, exhibiting high catalytic efficiency through the cooperative work of hydrogen bond/metal coordination and through soft–soft interactions/hard–hard interactions, respectively, are described. All the reactions presented here proceed under proton transfer conditions with perfect atom economy,[12] generating no reagent-derived waste. The hydrogen bond/metal coordination control of the stereochemical course of the reaction exerted by the RE metal/amide-based ligand catalyst allows for the use of high-

† Present address: *Institute of Microbial Chemistry, Tokyo; 3–14–23 Kamiosaki, Shinagawa-ku, Tokyo 141–0021, Japan.*

e-mail: nkumagai@bikaken.or.jp

ly coordinative substrates, which have not been a main subject of research in the field of asymmetric catalysis because of the difficulty in stereocontrol. The uniqueness of the flexible structure and intermolecular association of amide-based ligands in combination with RE metals has enabled the development of heterogeneous bimetallic asymmetric catalysts, asymmetric catalysts enabling a functional change in the course of a reaction, and an enantiodiscrimination originating from a molecular recognition function with high fidelity. Application to the efficient enantioselective synthesis of therapeutic candidates, such as AS-3201 and the β_3-adrenoreceptor agonist, using this catalytic system is also worthy of note. The effectiveness of a soft Lewis acid/hard Brønsted base catalyst to activate a Lewis basic functionality has identified the meritorious properties of allylic cyanides as carbon pronucleophiles, developing both α- and γ-addition of these compounds in a catalytic asymmetric manner under proton transfer conditions, constructing tetrasubstituted stereogenic carbon centers. This catalyst system allowed for the first example of catalytic and chemoselective generation of thioamide enolates under proton transfer conditions, leading to direct catalytic asymmetric Mannich-type and aldol reactions of thioamides with remarkable chemoselectivity.

1. Development of RE Metal/Amide-Based Ligand Catalysts

1.1. Catalytic Asymmetric Amination

1.1.1. Catalytic Asymmetric Amination of Succinimide Derivatives and Its Application to the Practical Synthesis of Ranirestat Electrophilic α-amination of carbonyl compounds is a useful transformation for installing an amino functionality adjacent to a carbonyl group to provide aminocarbonyl synthons with broad synthetic utility.[13,14] Although this specific transformation using azodicarboxylate as a formal "NH_2^+" reagent was discovered in 1954,[15—17] its enantioselective variants have only been found recently.[18—23] Our particular focus at the beginning of this project in 2006 was the establishment of a concise, practical, and enantioselective synthetic route to Ranirestat (AS-3201, **1**), a highly potent aldose reductase inhibitor.[24—26] Whereas almost all the other candidate aldose reductase inhibitors were withdrawn during the course of clinical development, **1** was identified as a structurally novel aldose reductase inhibitor bearing a spirosuccinimide entity exhibiting remarkable efficacy and safety.[24] **1** is orally available and is under late-stage clinical trials in the U.S. and Canada for the treatment of diabetic neuropathy. When we launched our study, the asymmetric synthesis of **1** relied on the optical resolution of racemic **2** through two cycles of recrystallization with cinchonidine, placing a severe limitation on the large-scale production of

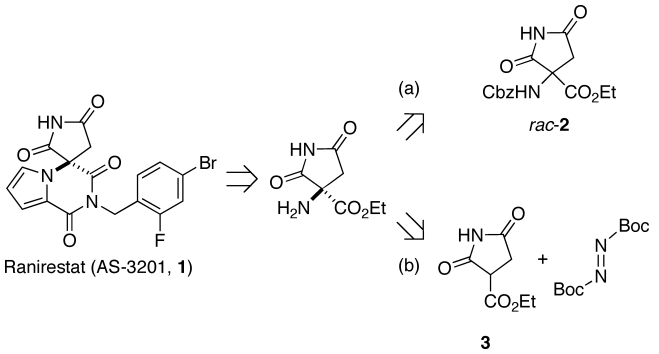

Chart 1. Retrosynthetic Analysis of Ranirestat (AS-3201, **1**)

this highly potent therapeutic candidate (Chart 1a).[24] The structural feature of **1** is a stereogenic tetrasubstituted carbon bearing an amino functionality, and its catalytic asymmetric construction is the obvious key to the practical synthesis of **1**. A retrosynthetic analysis of **1** indicated that the catalytic asymmetric amination of the succinimide derivative **3** was a viable approach to this end (Chart 1b).

Initially, we evaluated a set of known catalysts for the asymmetric amination of β-ketoesters using azodicarboxylates. However, none of these catalysts delivered the desired product **3** with satisfactory enantioselectivity. This is probably because of the highly coordinative nature and multiple coordination modes of **3**, which are undesirable properties for controlling the stereoselection in asymmetric catalysis, leading to unexpectedly poor enantioselectivity. These results prompted us to develop a new catalytic system that would be effective for such a highly coordinative substrate. We focused on a combination of RE metals and an amide-based ligand as a catalyst, where the RE metal would be surrounded by amide-based ligands to avoid an unfavorable coordination of **3** owing to the high coordinative nature of amides to RE metals.[27] We also anticipated that the high coordination number of the RE metals would allow for the additional coordination of **3** in a specific coordination mode. Exploration of the catalysts prepared from a combination of RE metals/amide-based ligands[28,29] showed that the amide-based ligand (*R*)-**4a** was a promising chiral ligand for catalytic asymmetric amination of **3**.[30] The synthesis of bis(2-hydroxyphenyl)amide (*R*)-**4a** is straightforward and easy to prepare in large quantities from commercially available *N*-*tert*-butoxycarbonyl (Boc)-D-valine without using column chromatography. The first-generation amination catalyst, prepared by mixing (*R*)-**4a** and $La(O^iPr)_3$ in a 2 : 1 ratio, promoted the asymmetric amination of **3** and di-*tert*-butyl azodicarboxylate in $CHCl_3$ in the presence of *N*,*N*-dimethylacetamide, affording the desired amination

Naoya Kumagai was born in 1978 and raised in Ibaraki, Japan. He received a BA in Pharmaceutical Sciences at the University of Tokyo in 2000. After receiving a PhD in Pharmaceutical Sciences at the University of Tokyo in 2005 under the supervision of Prof. Masakatsu Shibasaki, he pursued postdoctoral study in the laboratory of Prof. Stuart L. Schreiber at Harvard University, 2005—2006. He moved to Prof. Shibasaki's group as an assistant professor in 2006. He is currently a researcher at the Institute of Microbial Chemistry, Tokyo. His research interest is in the development of new methodologies in asymmetric catalysis and their applications to bioinspired dynamic processes.

Naoya Kumagai

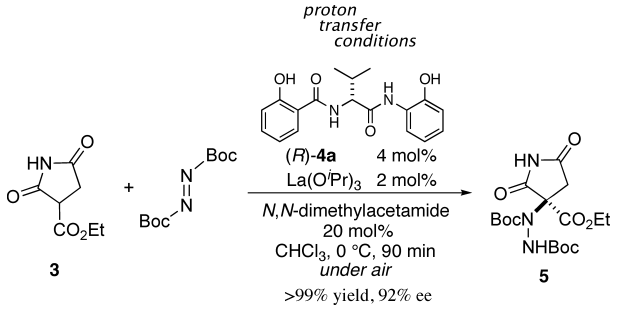

Chart 2. The First-Generation Amination Catalyst Comprised of $La(O^iPr)_3$/(*R*)-**4a**

product **5** in >99% yield and 92% ee (Chart 2). The reaction worked well with 2 mol% of catalyst loading under air, and **5** was successfully converted to **1** in an optically pure form after a five-step transformation and a single recrystallization.[25,31—33)]

Although the first-generation catalyst gave the amination product in high ee under proton transfer conditions, several concerns remained regarding its industrial application: 1) $La(O^iPr)_3$ is a very expensive chemical (US$224 for 3 g, Aldrich Chemicals, U.S.A.),[34)] and it is not available in bulk quantity, is unstable in the presence of moisture, and must be handled in an inert atmosphere before preparation of the catalyst; 2) a fluctuation in both the reactivity and enantioselectivity is occasionally observed, depending on the production batch of $La(O^iPr)_3$, likely because of the difference in the oligomeric state of the reagent; and 3) the use of $CHCl_3$ as a solvent must be avoided. These concerns prompted us to seek an alternative lanthanum source for the La/(*R*)-**4a** catalyst. Most lanthanum salts are hardly soluble in organic solvents and unfavorable for catalyst preparation. Based on the fact that nitrate anions enhance the solubility of lanthanide complexes,[35)] we turned our attention to the combined use of lanthanum salts and $^nBu_4N(NO_3)$. Eventually, $La(NO_3)_3\cdot 6H_2O$ was identified as the optimum lanthanum source for our specific purpose because of its relatively high solubility in AcOEt, its tolerance to moisture, and its availability in large quantities at low cost (US$443 for 500 g, Aldrich Chemicals, U.S.A.).[34)] The neutral nature of $La(NO_3)_3\cdot 6H_2O$ requires an additional base to promote the amination reaction, and the structure of the amine bases, including their stereochemistry, is a determining factor for enantioselectivity, implying that the amines are involved in the transition state. Assuming that two molecules of (*R*)-**4a** to lanthanum cation were needed to construct a favorable transition state architecture in the first-generation catalyst using $La(O^iPr)_3$, D-valine *tert*-butyl ester H–D-Val–O^{t}Bu, bearing the partial structure of (*R*)-**4a**, was used in combination with $La(NO_3)_3\cdot 6H_2O$/(*R*)-**4a**, and this catalytic system produced the amination product **5** with high catalytic efficiency, thereby establishing the second-generation catalyst. This ternary catalytic system allowed for a 100-g scale demonstration of the amination of **3** [$La(NO_3)_3\cdot xH_2O$, an even cheaper lanthanum source is also applicable], affording the hydrazine HCl salt in 96% yield (two steps), and 91% ee after the removal of the Boc groups under acidic conditions, which is used directly for the enantioselective synthesis of **1b** (Chart 3).[36,37)]

1.1.2. Catalytic Asymmetric Amination of *N*-Nonsubstituted α-Alkoxycarbonyl Amides Catalytic asymmetric amination of the *N*-nonsubstituted α-alkoxycarbonyl amides **6** allows for the efficient access to enantiomerically enriched α-amino-α-alkoxycarbonyl amides.[38)] However, there are no catalytic asymmetric transformations utilizing this class of substrates, likely because of: 1) the relatively high pK_a of the α-C–H proton compared with other active methylene compounds; 2) the competitive deprotonation of the α-C–H proton and the kinetically more labile amide N–H protons; and 3) the multiple coordination pattern of **6** leading to poor enantioselectivity. We anticipated that the $La(NO_3)_3\cdot 6H_2O$/(*R*)-**4a**/H–D-Val–O^{t}Bu ternary catalytic system would exhibit high catalytic performance, in which the coordination to a lanthanum cation and hydrogen bond would cooperatively activate **6** with excellent control of the stereochemical course of the reaction. Several control experiments revealed that the ternary catalytic system recognizes the α-alkoxycarbonyl amide motif with a *trans*-N–H proton as a privileged substructure, which appears in both succinimide derivatives **3** and **6**. Indeed, the catalytic asymmetric amination of **6** proceeded in a highly enantioselective manner with a range of substrates to produce α,α-disubstituted amino acid derivatives **7** bearing a tetrasubstituted stereogenic center (Table 1).[39)]

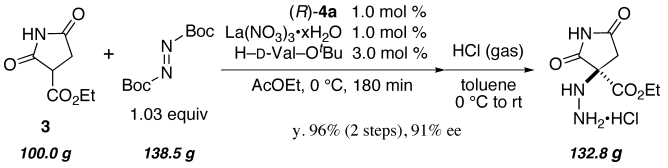

Chart 3. The Second-Generation Ternary Catalytic System Comprised of $La(NO_3)_3\cdot xH_2O$/(*R*)-**4a**/H–D-Val–O^{t}Bu

Mechanistic studies employing MS, NMR, and circular dichroism (CD) analysis, and Eyring plots, as well as several control and kinetic experiments suggested that the catalyst components of the ternary catalyst were in dynamic equilibrium between the associated and dissociated state, and a 1 : 1 : 1 ternary complex of $La(NO_3)_3\cdot 6H_2O$/(*R*)-**4a**/H–D-Val–O^{t}Bu was likely involved in the transition state (Fig. 1). All of the three components of the catalyst are indispensable, and the cooperative coordination to the lanthanum cation and hydrogen bond interactions are key to constructing the ternary complex and the specific recognition/activation of the highly coordinative nonprotected substrates **3** and **6**.

1.2. *anti*-Selective Catalytic Asymmetric Nitroaldol (Henry) Reaction The nitroaldol (Henry) reaction is a valuable and robust methodology for carbon–carbon bond-forming reactions that proceed under proton transfer conditions with perfect atom economy (Chart 4).[40—43)] Almost 100 years have passed since the discovery of the transformation before the reaction was rendered enantioselective in a catalytic manner in 1992 using a $LaLi_3$(binaphthoxide)$_3$ (LLB) catalyst.[44)] Since then, catalytic asymmetric nitroaldol reactions have emerged as a useful protocol for the rapid assembly of enantioenriched 1,2-nitro alkanols, which allows for direct access to synthetically versatile 1,2-amino alcohols. Although numerous catalysts for the catalytic asymmetric nitroaldol reactions of nitromethane have been found, progress toward catalytic enantio- and diastereoselective nitroaldol reactions using other nitroalkanes has been limited, except for

Table 1. Catalytic Asymmetric Amination of α-Alkoxycarbonyl Amides **6** Promoted by a $La(NO_3)_3 6H_2O$/(*R*)-**4a**/H–D-Val–O^{t}Bu Ternary Catalyst

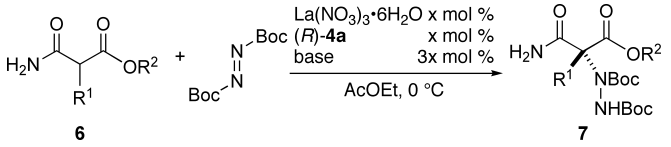

Entry	R^1	R^2		x	Product	Time (h)	Yield[a] (%)	ee (%)
1	Ph	Et	**6a**	10	**12a**	48	83	>99
2	Ph	Me	**6b**	10	**12b**	24	92	>99
3	4-FC_6H_4	Me	**6c**	10	**12c**	14	99	>99
4	4-FC_6H_4	Me	**6c**	3	**12c**	36	81	91
5	2-FC_6H_4	Et	**6d**	10	**12d**	48	45	94
6	4-$CF_3C_6H_4$	Me	**6e**	10	**12e**	14	94	>99
7	4-MeC_6H_4	Et	**6f**	10	**12f**	12	92	99
8	2-Naphthyl	Et	**6g**	10	**12g**	18	>99	>99
9	4-$MeOC_6H_4$	Et	**6h**	10	**12h**	48	88	99
10	4-$NO_2C_6H_4$	Et	**6i**	10	**12i**	10	>99	>99
11	4-$NO_2C_6H_4$	Et	**6i**	3	**12i**	36	84	90
12	3-Thienyl	Et	**6j**	10	**12j**	15	>99	99
13	3-Pyridyl	Et	**6k**	10	**12k**	12	70	>99
14	Me	Et	**6l**	10	**12l**	45	98	83

a) Isolated yield.

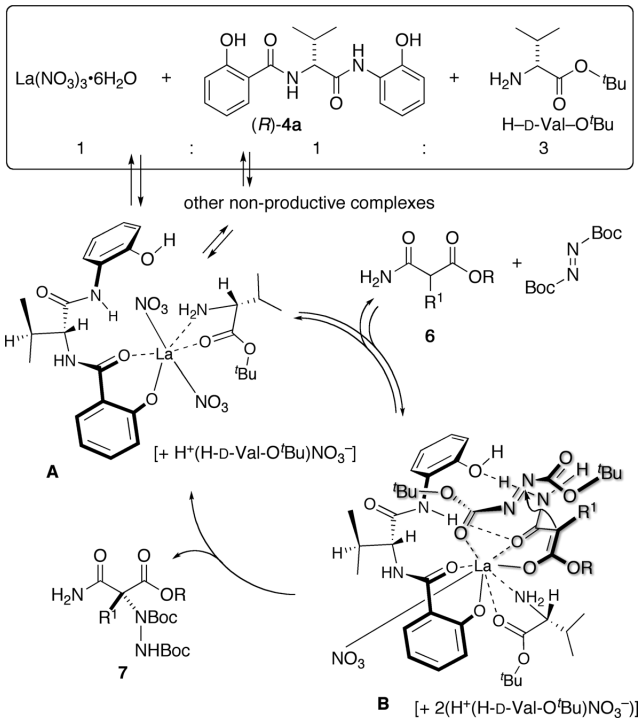

Fig. 1. Proposed Catalytic Cycle for the Second-Generation Catalytic Asymmetric Amination

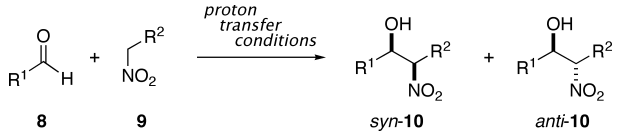

Chart 4. The Nitroaldol (Henry) Reaction

a few sporadic reports.[45—47] In particular, *anti*-diastereoselectivity in this transformation has remained a formidable task,[48—51] presumably because a simple chelation model prefers *syn*-diastereoselectivity (Fig. 2b). A rational approach to achieve high *anti*-diastereoselectivity was reported by Seebach *et al.* using silyl nitronates as an activated nucleophile, where the antiparallel orientation of a silyl nitronate and an aldehyde was proposed to explain the observed *anti*-diastereoselectivity (Fig. 2a).[52] We hypothesized that a heterobimetallic catalyst comprised of a chiral ligand with an appropriate spatial arrangement for two distinct metal coordination sites would provide a suitable chiral platform for the antiparallel transition state. In this catalyst design, each distinct metal cation, M_1 and M_2, works independently as a Lewis acid to activate an aldehyde and a Brønsted base (metal phenoxide) to form metal nitronates, respectively (Fig. 2c). We anticipated that an amide-based ligand bearing a binary metal coordination site linked by a stereogenic α-amino acid through two amide planes bearing aryl oxide functionality would provide a suitable three-dimensional architecture on complexation with an RE cation (M_1 as a Lewis acid) and an alkali metal cation (M_2OAr as a Brønsted base). A systematic screening of $RE(O^iPr)_3$, an alkali metal source, and amide-based ligand revealed that an Nd/Na heterobimetallic catalyst assembled using an amide-based ligand having a *meta*-oriented phenolic OH (*S*)-**4b** derived from L-leucine showed promising *anti*-selectivity (*anti*/*syn*=7.9/1) and enantioselectivity (53% ee) in the reaction of benzaldehyde (**8a**) and nitroethane (**9a**) (Chart 5a).[53,54] A fluorinated ligand (*S*)-**4c**, where an intramolecular hydrogen bond between a fluoro substituent and amide hydrogen was anticipated to restrict the rotation of the C–C single bond between the *m*-hydroxy phenyl group and amide, outperformed the parent ligand (*S*)-**4b** to afford the product **10aa** in 99% yield with higher stereoselectivity (*anti*/*syn*=>40/1, 84% ee) (Chart 5b).[55] During the catalyst preparation process, *i.e.*, mixing $Nd_5O(O^iPr)_{13}$, sodium hexamethyldisilazide (NaHMDS), and (*S*)-**4c** in tetrahydrofuran (THF) and nitroethane **9a**, an extensive white suspension was formed, leading us to identify an Nd/Na heterogeneous complex with an approxi-

mate molar ratio of Nd/(*S*)-**4c**/Na=1/0.96/1.8, confirmed by inductively coupled plasma (ICP) spectroscopy and X-ray fluorescence (XRF) spectroscopy.[56] The heterogeneous Nd/Na complex assembled by the amide-based ligand (*S*)-**4c** was isolated using centrifugation and could be stored for several months, exhibiting higher catalytic performance and stereoselectivity, reaching 98% ee. The *anti*-selective catalytic asymmetric nitroaldol reaction proceeded with a range of aldehydes **8** and functionalized nitroalkanes **9** using 1—6 mol% of catalyst, affording the corresponding 1,2-nitroalkanol in a highly *anti*-selective and enantioselective manner (Table 2). A large-scale demonstration of the nitroaldol reaction with the heterogeneous catalyst highlighted the synthetic utility of the present protocol. The nitroaldol reaction of 50 g of 4-benzyloxybenzaldehyde **7c** and **8a** (used as received from a commercial source) was run with 1 mol% of catalyst at −30 °C for 24 h, giving **10ca** in 76% yield with *anti*/*syn*=>40/1 and 98% ee (*anti*) after recrystallization of the crude mixture, which is a key intermediate for the potent β_3-adrenoreceptor agonist **11** (Chart 6).[57] This process is now under extensive investigation for industrial application in the bulk production of **11**.

1.3. Catalytic Asymmetric Nitro-Mannich (Aza-

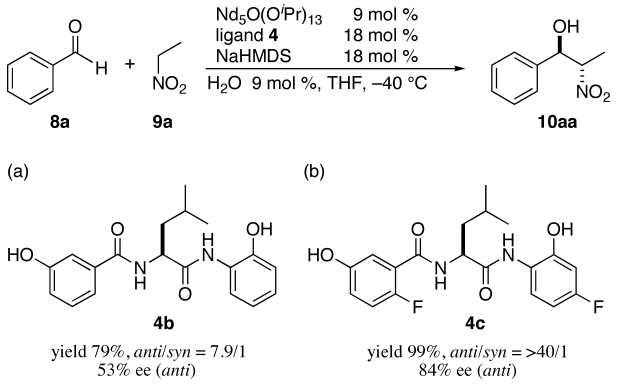

Chart 5. Identification of the Nd/Na/Amide-Based Ligand Heterobimetallic Catalyst

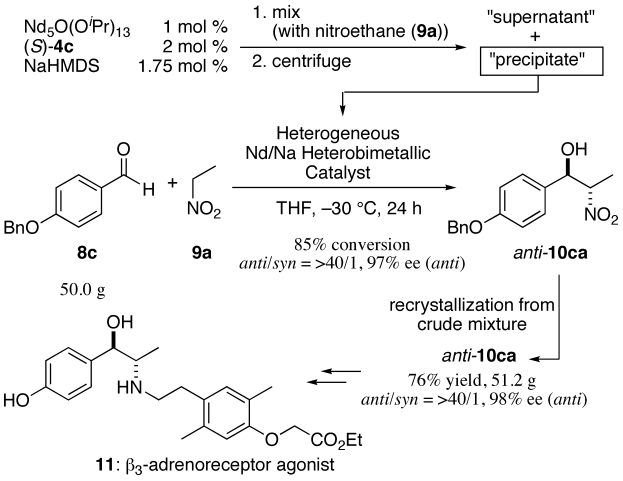

Chart 6. Large-Scale Demonstration of the *anti*-Selective Nitroaldol Reaction Promoted by a Heterogeneous Nd/Na Heterobimetallic Catalyst

Table 2. *anti*-Selective Catalytic Asymmetric Nitroaldol Reaction with the Nd/Na Heterobimetallic Heterogeneous Catalyst

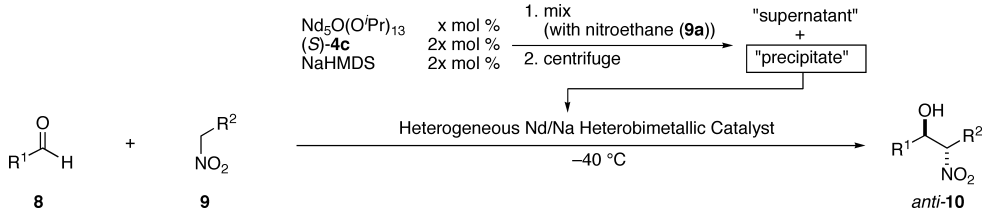

Entry	Aldehyde **8**		Nitroalkane **9**		equiv.	*x*	Solvent	Product	Time (h)	Yield[a] (%)	*anti*/*syn*[b]	ee (*anti*) (%)
	R^1=		R^2=									
1	Ph	**8a**	Me	**9a**	10	3	THF	**10aa**	20	99	>40/1	92
2[c]	Ph	**8a**	Me	**9a**	10	1	THF	**10aa**	20	96	>40/1	91
3	Ph	**8a**	Me	**9a**	3	3	THF	**10aa**	20	95	>40/1	93
4	Ph	**8a**	Me	**9a**	1.5	3	THF	**10aa**	20	91	33/1	89
5	2,4-$Me_2C_6H_3$	**8b**	Me	**9a**	10	3	THF	**10ba**	20	99	>40/1	98
6	4-$BnOC_6H_4$	**8c**	Me	**9a**	10	3	THF	**10ca**	20	89	>40/1	97
7	4-BrC_6H_4	**8d**	Me	**9a**	10	3	THF	**10da**	14	95	37/1	94
8	4-FC_6H_4	**8e**	Me	**9a**	10	3	THF	**10ea**	20	99	>40/1	97
9	4-NO_2	**8f**	Me	**9a**	10	3	THF	**10fa**	20	99	5.7/1	86
10	4-CN	**8g**	Me	**9a**	10	3	THF	**10ga**	20	88	15/1	94
11	4-$MeO_2CC_6H_4$	**8h**	Me	**9a**	10	3	THF	**10ha**	14	96	23/1	89
12	2-Furyl	**8i**	Me	**9a**	10	3	THF	**10ia**	20	99	13/1	82
13	*trans*-PhCH=CH	**8j**	Me	**9a**	10	3	THF	**10ja**	20	96	40/1	97
14	$PhCH_2CH_2$	**8k**	Me	**9a**	10	6	DME	**10ka**	20	99	4.9/1	77
15	^cHex	**8l**	Me	**9a**	10	6	DME	**10la**	22	92	8.3/1	95
16	$^nC_8H_{11}$	**8m**	Me	**9a**	10	6	DME	**10ma**	20	93	3.4/1	87
17	Ph	**8a**	Et	**9b**	10	3	THF	**10ab**	20	99	>40/1	90
18	4-FC_6H_4	**8e**	Et	**9b**	10	3	THF	**10eb**	20	93	19/1	90
19	Ph	**8a**	$TBSOCH_2$	**9c**	5	3	Et_2O	**10ac**	48	85	13/1	90
20	Ph	**8a**	$BnOCH_2$	**9d**	5	3	THF	**10ad**	48	75	19/1	95

a) Isolated yield. *b*) Determined by ^{1}H-NMR analysis. *c*) 1 mol % of NaHMDS was added to the Nd/Na heterobimetallic catalyst.

Henry) Reaction In our continuing program to expand the utility of the heterobimetallic bifunctional catalyst organized by the amide-based ligand (*S*)-**4c**, we envisioned developing a diastereo- and enantioselective nitro-Mannich (aza-Henry) reaction based on RE metal/alkali metal heterobimetallic catalysis.[58—61] This synthetic methodology assembles imines **12** and nitroalkanes **9** under proton transfer conditions, affording enantiomerically enriched β-nitroamines **13**. Facile reduction of the nitro functionality of the nitro-Mannich product to amines allowed for efficient access to synthetically versatile, optically active 1,2-diamines. The Nd/Na/(*S*)-**4c** heterogeneous heterobimetallic catalyst, which was identified as the optimum catalytic system for *anti*-selective asymmetric nitroaldol reactions, was employed for the asymmetric nitro-Mannich reaction of *N*-Boc imine **12a** and nitroethane **9a**, affording *anti*-**13aa** preferentially in 87% yield, albeit with poor stereoselectivity [*anti*/*syn*=3.7/1, 0% ee (*anti*)]. A new heterobimetallic entity comprising Yb/K/(*S*)-**4c** emerged as the optimum catalyst for the nitro-Mannich reaction through extensive binary metal screening (Table 3).[62]

Table 3. *anti*-Selective Catalytic Asymmetric Nitro-Mannich Reaction with a Yb/K Heterobimetallic Catalyst.

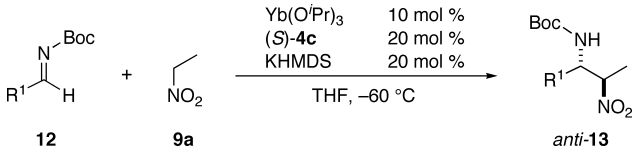

12 **9a** *anti*-**13**

Entry Entr	R^1		Product	Time (h)	Yield[a] (%)	*anti*/*syn*[b]	ee (%)
1	Ph	**12a**	**13aa**	22	80	18/1	73
2	2-Naph	**12b**	**13ba**	22	71	17/1	72
3	4-MeC_6H_4	**12c**	**13ca**	44	87	22/1	86
4	3-MeC_6H_4	**12d**	**13da**	20	76	13/1	75
5	4-MeOC_6H_4	**12e**	**13ea**	44	79	19/1	82
6	4-ClC_6H_4	**12f**	**13fa**	20	74	6.6/1	50
7	4-CFC_6H_4	**12g**	**13ga**	20	72	2.4/1	14

a) Isolated yield. *b*) Determined by ^{1}H-NMR of crude mixture.

1.4. Catalytic Asymmetric Mannich-Type Reaction

1.4.1. Development of *anti*- and *syn*-Selective Reactions Using α-Cyanoketones Catalytic asymmetric construction of an all-carbon quaternary stereogenic center under proton transfer conditions has attracted increasing attention due to the limited methodologies for this synthetic challenge.[63—66] An α-cyanocarbanion, with its minimal steric bias and its inherent nucleophilicity, is a suitable carbon nucleophile for the formation of a chiral quaternary carbon center.[67—69] We envisioned applying an RE/amide-based ligand catalytic system to a catalytic asymmetric Mannich-type reaction[70—73] of *N*-Boc imine **12** and α-cyanoketone **14** under proton transfer conditions, affording a densely functionalized product with a contiguous quaternary carbon and trisubstituted stereocenter **15** (Chart 7). When we began this project, there were several precedents for the catalytic asymmetric Mannich-type reaction using 1,3-dicarbonyl compounds as pronucleophiles generating quaternary stereogenic centers with 1,2-*syn* relative stereochemistry.[74—79] None of these examples, however, exhibited high *anti*-diastereoselectivity. In contrast to 1,3-dicarbonyl compounds, which coordinate to metal-based catalysts in a bidentate fashion, α-cyanoketones display a monodentate coordination mode, where it is difficult to control the stereochemical course of

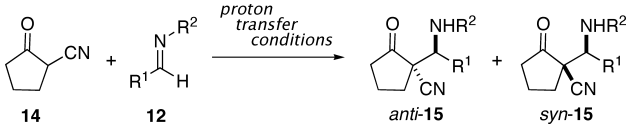

14 **12** *anti*-**15** *syn*-**15**

Chart 7. Catalytic Asymmetric Mannich-Type Reaction Generating an All-Carbon Quaternary Stereogenic Center under Proton Transfer Conditions

Table 4. *anti*-Selective Catalytic Asymmetric Mannich-Type Reaction Promoted by the Sc(O^{i}Pr)$_3$/**4a** Catalyst

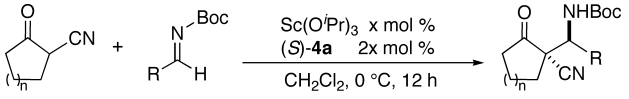

14 **12** *anti*-**15**

Entry	*x*	Cyanoketone *n*		Imine R		Product	Yield[a] (%)	*anti*/*syn*[b]	ee (*anti*) (%)
1[c]	5	1	**14a**	Ph	**12a**	**15aa**	90	94/6	94
2	2	1	**14a**	Ph	**12a**	**15aa**	93	93/7	91
3	5	2	**14b**	Ph	**12a**	**15ba**	92	95/5	91
4[d]	5	3	**14c**	Ph	**12a**	**15ca**	80	89/11	95
5	5	1	**14a**	2-MeC_6H_4	**12b**	**15ab**	90	91/9	93
6	5	1	**14a**	4-MeC_6H_4	**12c**	**15ac**	93	91/9	91
7	5	1	**14a**	2-Naphthyl	**12d**	**15ad**	97	90/10	94
8	5	1	**14a**	2-ClC_6H_4	**12e**	**15ae**	97	88/12	95
9	5	1	**14a**	4-ClC_6H_4	**12f**	**15af**	99	91/9	89
10	5	1	**14a**	2-FC_6H_4	**12g**	**15ag**	88	90/10	96
11	5	1	**14a**	2-MeOC_6H_4	**12h**	**15ah**	86	80/20	81
12	5	1	**14a**	4-MeOC_6H_4	**12i**	**15ai**	97	85/15	77
13	5	1	**14a**	2-Furyl	**12j**	**15aj**	94	75/25	82
14	5	1	**14a**	3-Thienyl	**12k**	**15ak**	98	93/7	83
15	5	1	**14a**	Ph$(CH_2)_2$	**12l**	**15al**	89	64/36	50

a) Isolated yield. *b*) Determined by ^{1}H-NMR of crude mixture. *c*) Average of two runs. *d*) Reaction time was 48 h.

the nucleophilic addition. This can be addressed by a cooperative activation/stereocontrol through the metal coordination and hydrogen bond exerted by an RE/amide-based ligand catalysis. Evaluation of a series of RE/amide-based ligand (*S*)-**4a** catalysts in the reaction of *N*-Boc imine **12** and 2-cyanocycloalkanones **14** revealed that the Sc(O^{i}Pr)$_3$/(*S*)-**4a** catalyst promoted the desired Mannich-type reaction to deliver the desired *anti*-product **15** with high enantioselectivity with 2—5 mol% of catalyst loading (Table 4).[80—82] Of particular note is that the Sc(O^{i}Pr)$_3$/(*S*)-**4a** catalyst did not form a distinct structure, on the basis of ^{1}H-NMR analysis, which is likely because several complexation patterns are possible from the structural flexibility and the monodentate coordination mode of the two phenolic hydroxyl groups of (*S*)-**4a**. The high stereoselectivity would be rationalized by assuming a well-organized association in the transition state from a nonordered reaction mixture ensemble. The nondefined structure of the Sc(O^{i}Pr)$_3$/(*S*)-**4a** catalyst may indicate that the RE/(*S*)-**4a** catalytic system retains the potential to provide a catalyst with a different structural motif from a different reaction ensemble. This hypothesis prompted us to explore the possibility of structural/functional modifications of the catalyst using this reaction system. In our search for other RE/(*S*)-**4a** catalysts, we identified that the Er(O^{i}Pr)$_3$/(*S*)-**4a** catalyst displayed a remarkable diastereoselectivity reversal compared with the Sc(O^{i}Pr)$_3$/(*S*)-**4a** catalyst, giving *syn*-**15** with 99% ee under otherwise identical reaction conditions (Chart 8).[83—85] An enhanced catalytic activity was observed compared with the Sc(O^{i}Pr)$_3$/(*S*)-**4a** catalyst, allowing the reaction to take place with a range of imines **12**, reaching completion after 1 h of stirring in ether at 0 °C with 2 mol% of catalyst (Table 5). Of prime importance in the present catalytic system is the origin of the diastereoswitching. Clear differences in the CD spectrum of the Sc(O^{i}Pr)$_3$/(*S*)-**4a** and Er(O^{i}Pr)$_3$/(*S*)-**4a** catalyst suggested that a chiroptically different RE/(*S*)-**4a** assembly developed in each catalytic system. Because of the exquisite combination of factors, 1) the structural flexibility of the amide-based ligand (*S*)-**4a**; 2) the high coordination number of the RE; and 3) the possibility of various coordination patterns of the RE, RE/(*S*)-**4a** provided chiroptically different asymmetric catalysts in response to the properties of the RE used, consequently affording *anti* and *syn* products with a high enantioselectivity under otherwise identical conditions.

1.4.2. Structural Dynamics and Functional Diversity of the RE/(*S*)-4a Catalyst Enantioselective catalysts are usually designed to exert a single function under a single set of conditions in a single reaction flask. In some cases, the same catalyst can give rise to different products under an alternative set of conditions. However, it is rare for a single metal-based or organocatalyst to be able to promote multiple, highly enantioselective transformations within the same flask in response to an external signal similarly to highly sophisticated proteins and functional polypeptide-based biomacromolecules.[86—90] A particularly intriguing feature of functional proteins is the seamless linking of their structural dynamics and their functional diversity, namely, that a structural change leads to a turning on and a turning off of their function or results in them acquiring another function, en-

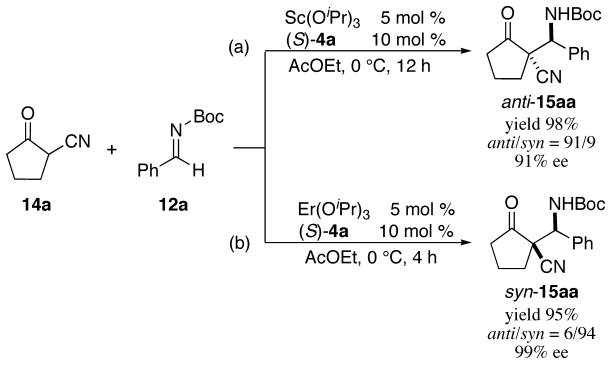

Chart 8. Diastereoswitching in the Catalytic Asymmetric Mannich-Type Reaction

Table 5. *syn*-Selective Catalytic Asymmetric Mannich-Type Reaction Promoted by the Er(O^{i}Pr)$_3$/(*S*)-**4a** Catalyst

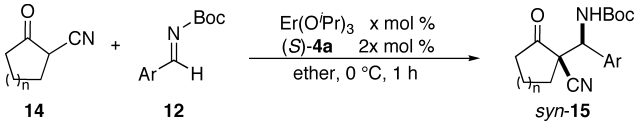

Entry	*x*	Cyanoketone *n*		Imine Ar		Product	Yield[a] (%)	*anti*/*syn*	ee (*syn*) (%)
1	2	1	**14a**	Ph	**12a**	**15aa**	92	6/94	95
2[b]	1	1	**14a**	Ph	**12a**	**15aa**	99	15/85	98
3[c]	5	2	**14b**	Ph	**12a**	**15ba**	97	13/87	97
4[c]	5	3	**14c**	Ph	**12a**	**15ca**	79	30/70	94
5	2	1	**14a**	2-MeC_6H_4	**12b**	**15ab**	99	5/95	99
6	2	1	**14a**	4-MeC_6H_4	**12c**	**15ac**	86	5/95	97
7[d]	2	1	**14a**	2-Naphthyl	**12d**	**15ad**	96	7/93	92
8	2	1	**14a**	2-ClC_6H_4	**12e**	**15ae**	99	4/96	99
9	2	1	**14a**	4-ClC_6H_4	**12f**	**15af**	95	5/95	91
10	2	1	**14a**	2-FC_6H_4	**12g**	**15ag**	91	7/93	99
11	2	1	**14a**	2-MeOC_6H_4	**12h**	**15ah**	99	4/96	99
12	2	1	**14a**	4-MeOC_6H_4	**12i**	**15ai**	82	4/96	92
13	2	1	**14a**	2-Furyl	**12j**	**15aj**	99	7/93	84
14	2	1	**14a**	3-Thienyl	**12k**	**15ak**	99	4/96	96

a) Isolated yield. *b*) Reaction time was 3 h. *c*) Reaction time was 20 h. *d*) CH_2Cl_2 was used as solvent.

abling the regulation of timely intra- and extracellular events to progress with an elegant synergy.[91—93] With RE/(*S*)-**4a** catalysts being effective for catalytic asymmetric Mannich-type reactions exhibiting diastereoswitching in response to the RE of choice, we attempted to link the structural dynamics and functional switching of an artificial catalyst, through which we would demonstrate diastereoselectivity switching during the course of a reaction in a single flask.

The Mannich-type reaction of **12a** and **14a** with a catalyst comprising $Sc(O^iPr)_3/Er(O^iPr)_3/(S)$-**4a**=1 : 1 : 4 afforded the *anti*-product **15aa** preferentially with an 88% ee (Chart 9), which is comparable with that obtained using the standard *anti*-selective catalyst $Sc(O^iPr)_3/(S)$-**4a** ($Sc(O^iPr)_3/(S)$-**4a**=1 : 2) (Table 4, Entry 1). CD analysis and various control experiments suggested that the $Sc(O^iPr)_3/(S)$-**4a** catalyst was preferentially formed over the $Er(O^iPr)_3/(S)$-**4a** catalyst in mixed-metal conditions, affording a similar reaction output to that of the $Sc(O^iPr)_3/(S)$-**4a** catalyst alone. Based on the fact that the association of $Sc(O^iPr)_3/(S)$-**4a** and $Er(O^iPr)_3/(S)$-**4a** was not kinetically stable, and that (*S*)-**4a** was involved in a dynamic exchange with Sc^{3+} and Er^{3+} cations, we set out to demonstrate a unidirectional catalyst modification during the course of the reaction. We designed the reaction system as follows. 1) A Mannich-type reaction of **14a** (2.4 eq) and **12e** (1.0 eq) was conducted using a $Er(O^iPr)_3$: (*S*)-**4a**=1 : 4 catalyst ($Er(O^iPr)_3$=2.5 mol% and (*S*)-**4a**=10 mol%) to form *syn*-**15ae**; 2) Then, $Sc(O^iPr)_3$ (2.5 mol%) was added to modify the catalyst structure, and another imine **12a** (1.0 eq) was introduced to afford *anti*-**15aa** (Chart 10a). The catalyst switched to engage in an *anti*-selective reaction. In this process, the structure of the catalyst changed in response to the property of the RE, providing both *syn*- and *anti*-products in a controlled fashion in a single flask. The structural change of the catalyst was monitored using CD analysis of the reaction mixture as illustrated in Chart 10. This process was also operative in the reaction of other sets of imine **12** and cyanoketones **14** (Chart 10b, c). These results are indicative of a timely functional change of the artificial asymmetric catalyst through a dynamic structural modification.

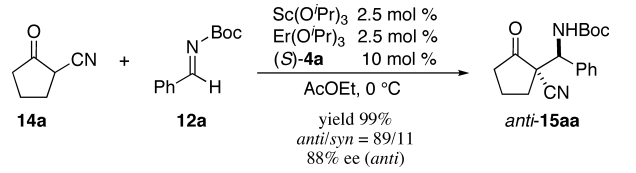

Chart 9. Catalytic Asymmetric Mannich-Type Reaction Promoted by a $Sc(O^iPr)_3/Er(O^iPr)_3/(S)$-**4a**=1 : 1 : 4 Catalyst

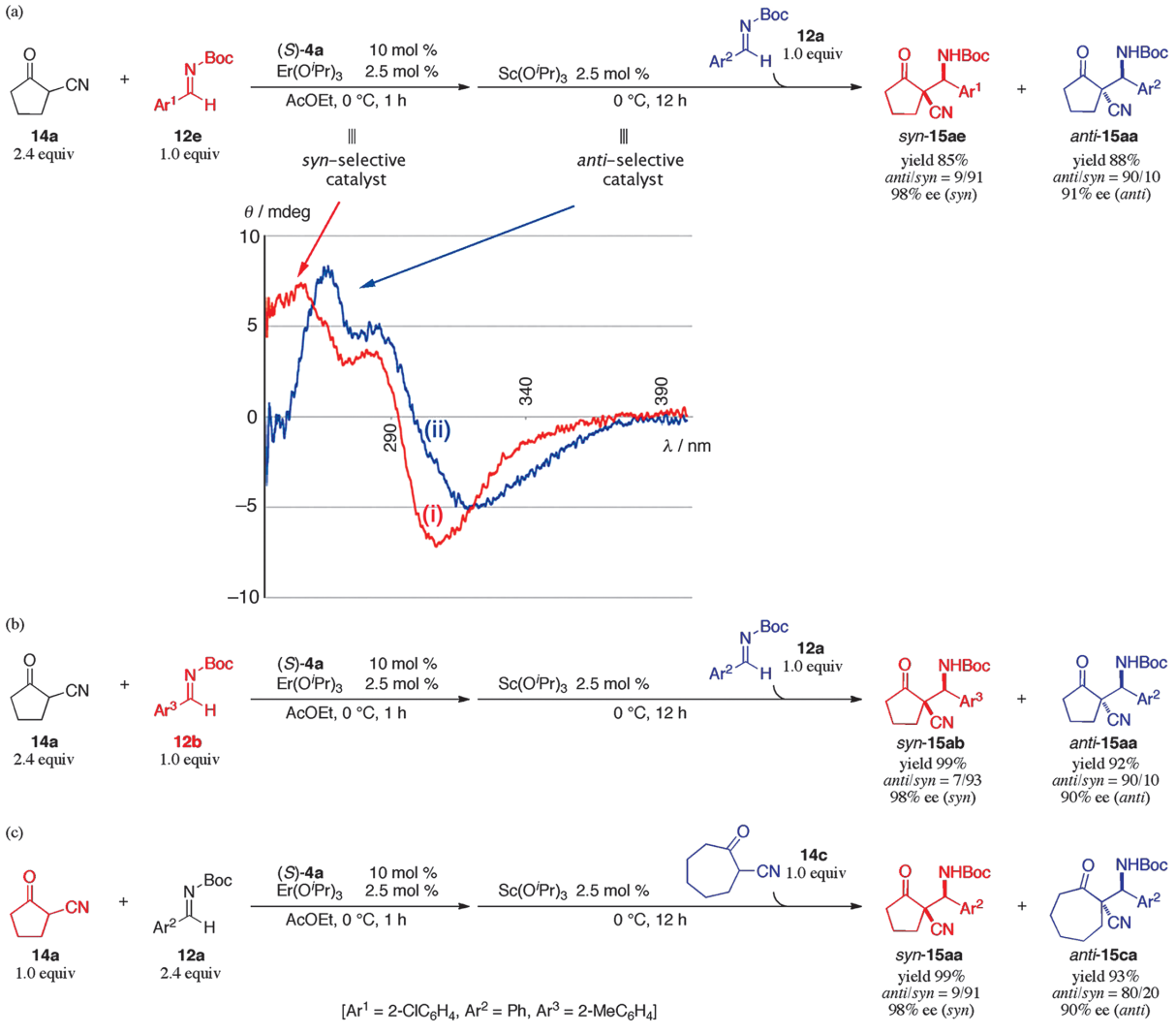

Chart 10. Dynamic Structural and Functional Changes of the RE/(*S*)-**4a** Catalyst in an Asymmetric Mannich-Type Reaction

1.5. Catalytic Asymmetric Conjugate Addition The utility of α-cyanoketones **14** as pronucleophiles for the construction of an all-carbon quaternary stereogenic center was further expanded by the development of a catalytic asymmetric conjugated addition. Recent advances in this field have revealed that the enantioselective addition of active methane pronucleophiles to electron-deficient alkenes is a highly versatile and atom-economical strategy for producing a class of compounds bearing functional groups that are amenable to subsequent manipulation (Chart 11).[94—98] The RE/(*S*)-**4a** complex, which was qualified as an effective catalytic system for the activation/stereocontrol of α-cyanoketones **14** in asymmetric Mannich-type reactions in the previous section, was evaluated in an asymmetric conjugate addition with vinyl ketones **16** to afford enantioenriched 1,5-dicarbonyl compounds **17**. The $Y(O^iPr)_3$/(*S*)-**4a**=1 : 2 catalyst emerged as the optimum catalyst for this specific transformation, promoting the reaction with 5 mol% of catalyst loading for vari-

Table 6. Catalytic Asymmetric Conjugate Addition of α-Cyanoketone **14** and Vinyl Ketone **16** Promoted by a $Y(O^iPr)_3$/(*S*)-**4a** Catalyst

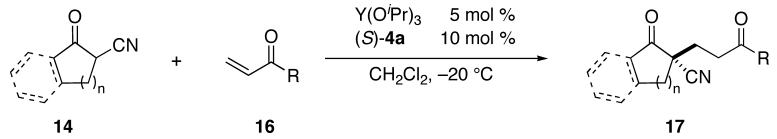

Entry	Cyanoketone	Enone	Product	Time (h)	Yield[a]	ee (%)
1	**14a**	**16a**	**17aa**	24	82	97
2	**14a**	**16b**	**17ab**	24	80	81
3	**14a**	**16c**	**17ac**	24	93	98
4[b]	**14a**	**16c**	**17ac**	24	83	97
5	**14a**	**16d**	**17ad**	24	82	87
6	**14a**	**16e**	**17ae**	24	80	93
7	**14a**	**16f**	**17af**	24	84	91
8	**14a**	**16g**	**17ag**	36	80	95
9[c]	**14a**	**16h**	**17ah**	24	75	90
10	**14a**	**16i**	**17ai**	24	79	94
11	**14a**	**16j**	**17aj**	24	89	97
12	**14a**	**16k**	**17ak**	24	60	95
13	**14a**	**16l**	**17al**	24	88	86
14	**14a**	**16m**	**17am**	24	98	84
15	**14a**	**16n**	**17an**	48	54	69
16	**14b**	**16a**	**17ba**	48	64	86
17	**14c**	**16a**	**17ca**	48	73	95
18	**14d**	**16a**	**17da**	24	82	70
19	**14e**	**16a**	**17ea**	48	48	88

a) Isolated. *b*) 1.1 g of **16c** was used. *c*) Yield was determined by ^{1}H-NMR analysis.

ous α-cyanoketones **14** and vinyl ketones **16** (Table 6).[99] Phenyl-fused cyanoketones **14d**, **e** were also applicable in this process. The product **17ac**, having a 1,5-dicarbonyl and a 2-cyano moiety, could be converted to two different bicyclic systems of bicyclo[3.3.0] **18ac** and spiropiperidine entities **19ac** *via* a chemoselective intramolecular cyclization (Chart 12).

1.6. Solvent-Dependent Self-Discrimination of Amide-Based Ligands

1.6.1. Association Property and Self-Discrimination of 4a Recently, considerable attention has been devoted to supramolecular chemistry that can produce a diverse array of assembled molecular architectures by harnessing various noncovalent inter- and intramolecular interactions.[100—104] In the NMR spectrum of enantiopure (*S*)-**4a** in chloroform-d_3, the chemical shift of the NH and OH protons, and also the aromatic CH protons, was variable depending on the concentration of the sample. This result suggests that extensive intermolecular interactions between **4a** molecules occur through hydrogen bonds. In our continuing effort to expand the utility of the amide-based ligand **4a**, we found that mixing a 0.1 M solution of (*S*)-**4a** and (*R*)-**4a** in a halogenated solvent like CH_2Cl_2 or $CHCl_3$ immediately gave rise to a thick suspension, while this was not the case for AcOEt, THF, or MeOH (Chart 13).[105] The isolated insoluble material was a racemate of **4a** with a much higher melting point (172 °C) than enantiopure **4a** (123—124 °C), suggesting that it was not a conglomerate, but a racemic compound,[106,107] as revealed by X-ray crystallographic analysis. To delineate the origin of the preferential heterochiral aggregation of **4a** and its solvent dependency, crystals of racemic **4a** were grown in either $CHCl_3$ (where extensive heterochiral aggregation was observed) or AcOEt/*n*-pentane (where no heterochiral aggregation was observed). As illustrated in Fig. 2, a regular zigzag alternating *S*/*R* array of association through hydrogen bonds was observed in the crystal structure of the racemate obtained from $CHCl_3$, which were laterally associated with each other to form a highly insoluble aggregate. On the other hand, a perusal of the crystal structure of the racemate from AcOEt/*n*-pentane led to the identification of an alternating *SS*/*RR* array, resulting in a significant difference in the solubility of racemic **4a**.

1.6.2. Self-Discrimination of 4a from an Ensemble of Eight Different Molecules Because the heterochiral association of **4a** appeared to originate from the hydrogen bond network connecting the characteristic bis(2-hydroxyphenyl)-diamide framework, we directed our attention to the possibility of the specific aggregation of (*S*)-**4a** and (*R*)-**4a** in an ensemble of structurally related molecules **4a**, **d**—**i** (Fig. 3a). A monoester analogue **4d**, bearing a salicylate moiety instead of salicylamide, did not form an insoluble heterochiral aggregate of **4d** on mixing (*R*)-**4d** and (*S*)-**4d** in CH_2Cl_2, indicating that the diamide substructure of the α-amino acid is crucial for the construction of the *S*/*R* alternating array found in the heterochiral aggregate of **4a**. Therefore another ester analogue, (*S*)-**4e**, deoxy analogues (*S*)-**4f** and (*S*)-**4g**, and analogues (*S*)-**4h** and (*S*)-**4i** with an appended methylene group were prepared and investigated for manifestation of the self-discrimination of **4a** in a closely related set of different molecules (Fig. 3b). On addition of a 0.1 M CH_2Cl_2 solution of (*R*)-**4a** (500 μl, 50 μmol) to a mixed solution of (*S*)-**4a**, (*S*)-**4d**, (*S*)-**4e**, (*S*)-**4f**, (*S*)-**4g**, (*S*)-**4h**, and (*S*)-**4i** (49±1 μmol each) in CH_2Cl_2 to develop an ensemble of eight molecules in equimolar amounts (Fig. 3c, blue bars), the clear solution gradually changed to form a thick suspension. After stirring for 48 h at 25±1 °C, the suspension was filtered, and the insoluble material was analyzed using HPLC. The insoluble material was comprised of a significant amount of (*S*)-**4a** and (*R*)-**4a** in an almost 1 : 1 ratio with trace amounts of other compounds, indicating the high fidelity of the self-discrimination of **4a** (Fig. 3c, red bars).

1.6.3. Large Nonlinear Effect in Asymmetric Catalysis The heterochiral aggregation of **4a** produced a strong asymmetric amplification of the solution ee value from an initial sample of **4a** with a low ee value.[108,109] Because **4a** serves as a chiral ligand in catalytic asymmetric reactions on complexation with an RE, as described above, we proceeded to demonstrate a large nonlinear effect in the catalytic asymmetric Mannich-type reaction of 2-cyanocyclopentanone (**14a**) and imine **12a**. A thick suspension developed when a sample of (*S*)-**4a** in 10% ee was stirred in CH_2Cl_2/*n*-hexane

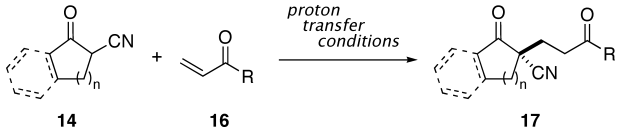

Chart 11. Catalytic Asymmetric Conjugate Addition under Proton Transfer Conditions

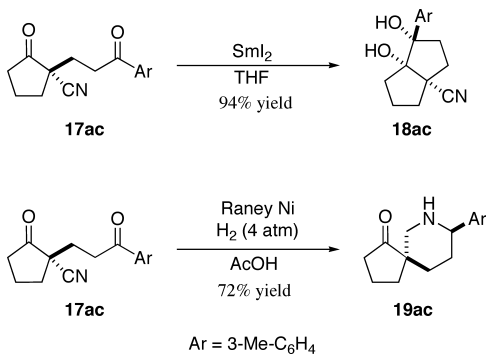

Chart 12. Catalytic Asymmetric Conjugate Addition under Proton Transfer Conditions

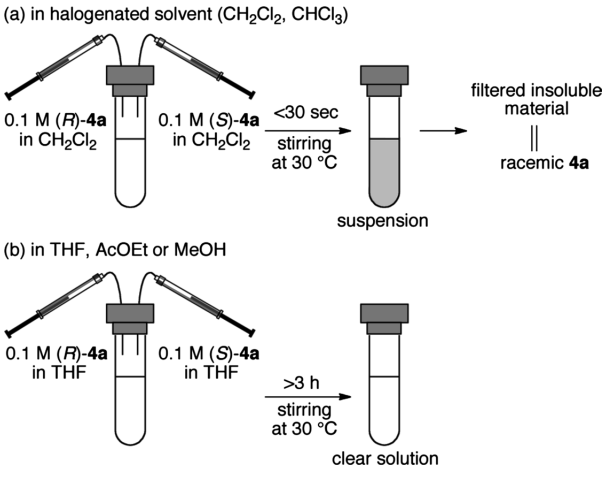

Chart 13. Solvent-Dependent Heterochiral Aggregation of **4a**

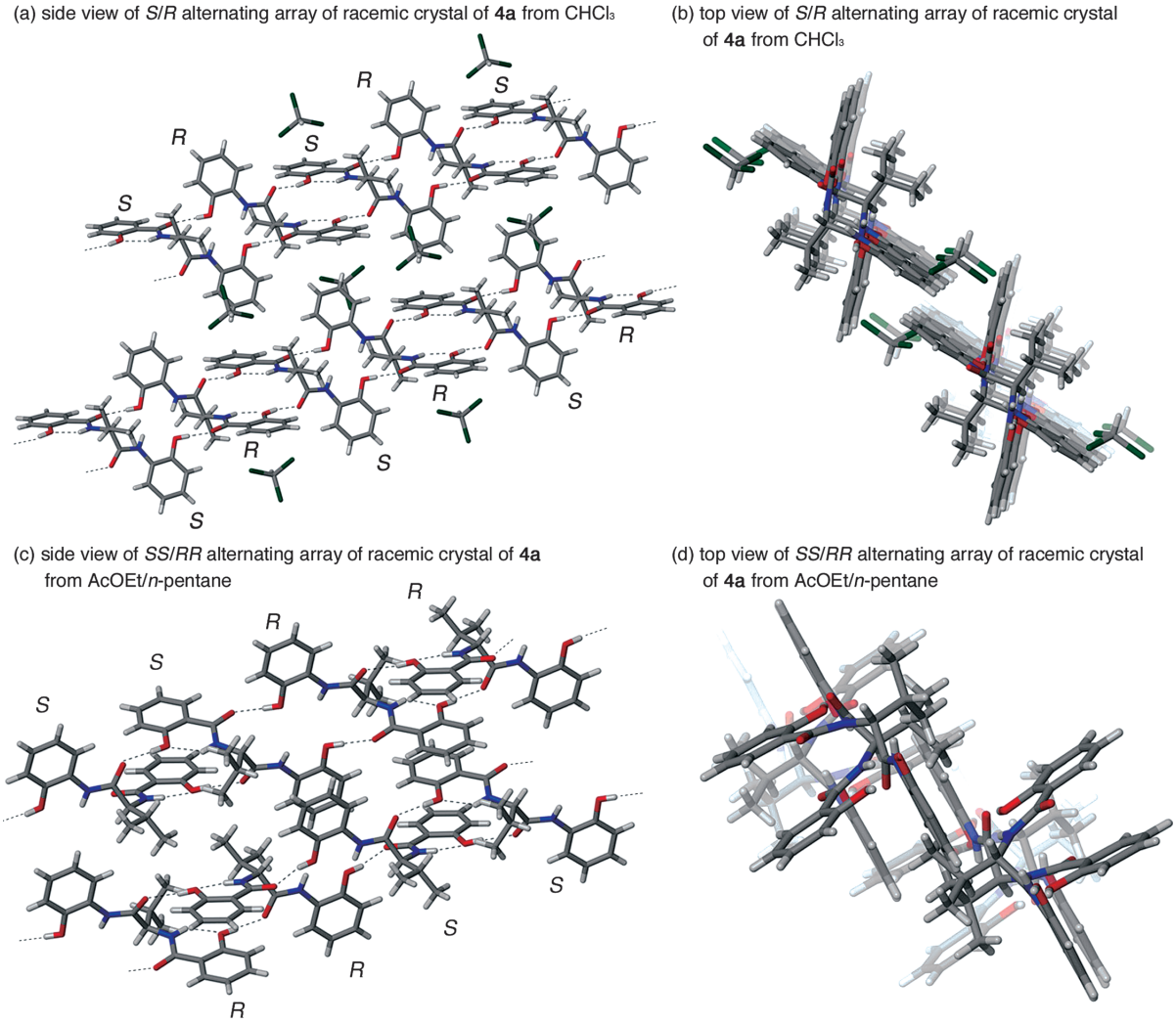

Fig. 2. Partial Structure of the *S*/*R* Alternating Array of a Racemic Crystal of **4a** Obtained from $CHCl_3$ (a) and (b), and That of the *SS*/*RR* Alternating Array of a Racemic Crystal of **4a** Obtained from AcOEt/*n*-Pentane (c) and (d)

(a) and (c) show the side view of the array of each crystal, showing the hydrogen bond network (dashed line). (b) and (d) show the top view of the array of each crystal. Key: carbon=dark gray; hydrogen=light gray; nitrogen=blue; oxygen=red; and chlorine=green.

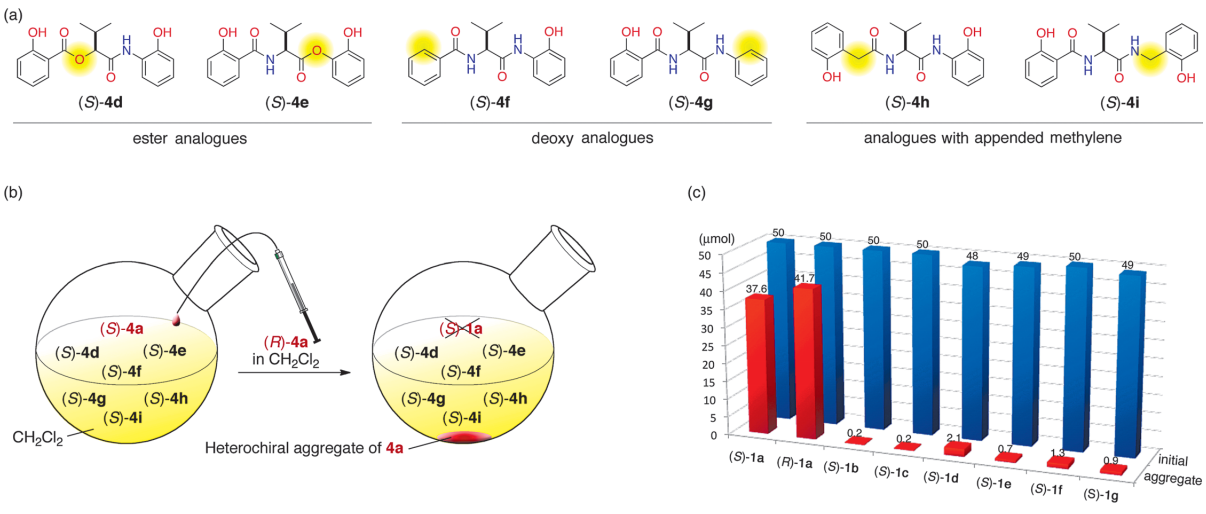

Fig. 3. (a) Structurally Related Bis(2-hydroxyphenyl)diamides **4d**—**i**; (b) Self-Discrimination of **4a** in an Ensemble of Eight Structurally Related Molecules; (c) Blue Bars=Initial Amount of Each Molecule, and the Red Bars=Amount of Each Molecule after Self-Discrimination of (*R*)-**4a** and (*S*)-**4a** from the Ensemble of Eight Molecules

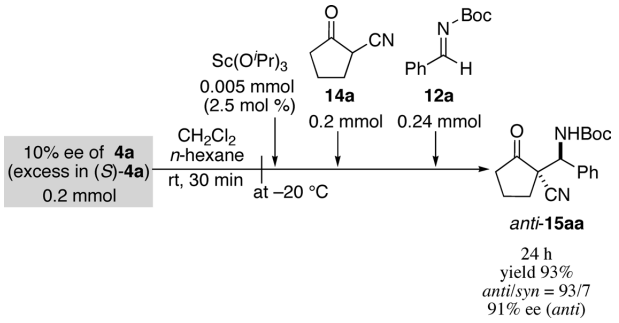

Chart 14. Catalytic Asymmetric Mannich-Type Reaction with a Low ee Sample of **4a**

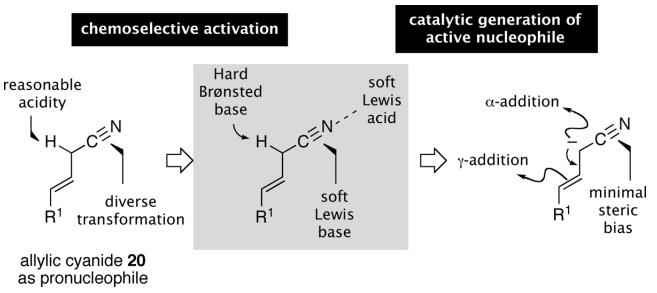

Fig. 4. Catalytic Generation of an Active Nucleophile from Allylic Cyanides **20** with a Soft Lewis Acid/Hard Brønsted Base Cooperative Catalyst

for a period of 30 min (Chart 14). Subsequent addition of Sc(O^{i}Pr)$_3$, **14a**, and **12a** at −20 °C afforded *anti*-**15aa** in 93% yield with *anti*/*syn*=93/7 and 91% ee, exhibiting a stereoselectivity comparable with that obtained using enantiopure (*S*)-**4a** (Table 4, Entry 1).[80]

2. Catalytic Activation of Soft Lewis Basic Pronucleophiles for Asymmetric C–C Bond Formation under Proton Transfer Conditions

2.1. Allylic Cyanides as Pronucleophiles The coupling of carbon nucleophiles with carbonyl groups and their related electrophilic C=X functionality in an enantioselective manner is a fundamental tool in organic synthesis for the construction of a carbon skeleton with a stereogenic center. Conventionally, preactivated carbon pronucleophiles, such as organometallic reagents or metalated enolates, are widely utilized with the concomitant generation of more than a stoichiometric amount of undesired waste. The catalytic generation of carbon pronucleophiles through proton transfer and subsequent integration into asymmetric carbon–carbon bond formation is increasingly recognized as a more advantageous strategy, because it provides a near ideal atom-economical process with minimal waste generation. Over the last decade, there have been considerable advances in this area, making the use of pronucleophiles such as ketones, aldehydes,[110—118] and ester equivalents[119—123] feasible. Alkylnitriles constitute a unique class of carbon pronucleophiles that are frequently utilized in various organic synthetic routes. From a synthetic viewpoint, alkylnitriles are stable, easy to handle, and have the same oxidation state as carboxylic acid, which enables a facile transformation into a range of functionalities of interest. Despite these favorable properties of alkylnitriles, there have been few attempts at catalytically generating nucleophiles from alkylnitrile, most likely because of its low acidity (pK_a=31.3 in dimethyl sulfoxide (DMSO)[124] and 28.9 in H_2O[125]), which poses a severe limitation on the chemoselective deprotonation of alkylnitrile pronucleophiles in the presence of carbonyl-type electrophiles.[126—130] In this context, our particular interest was directed towards the use of allylic cyanides **20**[131—133] as nitrile-based pronucleophiles because: 1) the unique linear topology of nitriles poses minimal steric bias, making them well suited to a highly congested transition state for the construction of tetrasubstituted carbon centers; 2) the soft Lewis basic character of the nitrile functionality allows for a chemoselective activation with a soft Lewis acid through a specific soft–soft interaction[134,135]; 3) the presence of an adjacent double bond lowers the acidity of the

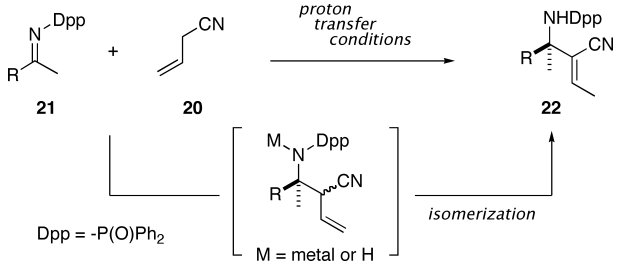

Chart 15. Direct Catalytic Asymmetric Addition of Allylic Cyanides **20** to Dpp-Ketoimines **21**

α-proton (pK_a=21.1 in DMSO)[136] favorable to catalytic deprotonation; 4) the allylic double bond enables γ-addition as well as α-addition, serving as an ambident pronucleophile; and 5) they can be viewed as a masked carboxylic acid derivative or amine, which promises a diverse transformation of the reaction product (Fig. 4). On the basis of this analysis, we envisioned that a cooperative catalyst comprised of a soft Lewis acid and a hard Brønsted base would provide a potential solution for the chemoselective activation of allylic cyanides **20** to integrate them into a catalytic asymmetric reaction that proceeds under proton transfer conditions.

2.1.1. Direct Catalytic Asymmetric Addition of Allylic Cyanides to Ketoimines The catalytic enantioselective construction of a stereogenic tetrasubstituted carbon *via* intermolecular carbon–carbon bond-forming reactions remains an intriguing challenge in asymmetric catalysis. Catalytic asymmetric additions to ketoimines using active organometallic nucleophiles have been developed recently as a new entry in this category, albeit with the concomitant generation of unwanted waste derived from organometallic reagents. However, the same transformation *via* proton transfer through the catalytic generation of active nucleophiles from otherwise inactive pronucleophiles is an obviously more advantageous protocol that has been rarely explored in this class of reactions, except for HCN[137—140] or the highly active α-alkoxycarbonylketoimines. In this context, we envisioned the direct catalytic asymmetric addition of allylic cyanides **20** to *N*-diphenylphosphinoyl (Dpp) ketoimines **21**,[141] exploiting the favorable properties of the cyanide-based pronucleophiles mentioned above (Chart 15).

An exquisite combination of cationic [Cu(CH$_3$CN)$_4$]ClO$_4$ as a soft Lewis acid, 1,2-bis((2*R*,5*R*)-2,5-diphenylphospholano) ethane ((*R*,*R*)-Ph-BPE) as a chiral bisphosphine ligand, and Li(OC$_6$H$_4$-*p*-OPh) as a hard Brønsted base enabled the catalytic generation of an active nucleophile and the subse-

quent α-addition to ketoimines **21**, affording the enantioenriched α,β-unsaturated nitriles **22** bearing a tetrasubstituted stereogenic center after spontaneous isomerization of the terminal olefin.[142] The use of other soft Lewis acidic cationic metals, such as $[Pd(CH_3CN)_4](BF_4)_2$ or $[Ag(CH_3CN)_4](BF_4)$, resulted in poor catalytic efficiency, confirming that Cu was the best soft Lewis acid for the activation of **20**. The substrate generality of the present protocol is summarized in Table 7. The reaction of a series of aryl methyl ketoimines **21** and allyl cyanide **20a** proceeded smoothly using 5—10 mol% of the cooperative catalyst to give the *Z* product preferentially with high enantioselectivity (Table 7, entries 1—6). Ketoimines with heteroaromatics and aliphatic ketoimines were also suitable substrates exhibiting high stereoselectivity (entries 7—11). Crotyl cyanide **20b** required an extended reaction time to give diastereomeric α-adducts, which isomerized to afford **22cb** with high *Z* selectivity on treatment with DBU at room temperature (entry 12). The reaction without $[Cu(CH_3CN)_4]ClO_4$ provided a poor conversion, verifying that a soft Lewis acid is essential for promoting the desired reaction.

2.1.2. Direct Catalytic Asymmetric Addition of Allyl Cyanide to Ketones Various methodologies based on the addition of preactivated organometallic nucleophiles to ketones have been developed for the catalytic asymmetric synthesis of enantioenriched tertiary alcohols, which are in high demand for broad utility in organic synthesis.[143—147] The highly congested transition state necessitates the use of highly active organometallic reagents, accompanied by the inevitable generation of more than stoichiometric amounts of unwanted waste. Catalytic generation of an active nucleophile by deprotonation coupled with a subsequent asym-

Table 7. Direct Catalytic Asymmetric Addition of Allylic Cyanides **20** to Ketoimines **21** Promoted by a Soft Lewis Acid/Hard Brønsted Base Cooperative Catalyst

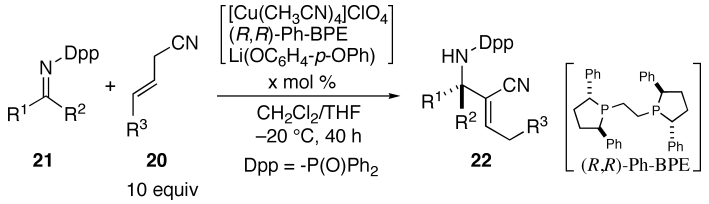

Entry	Ketoimine		Allylic cyanide		*x*	Product	Yield[a] (%)	*E*/*Z*[b]	ee (%)
1[c]	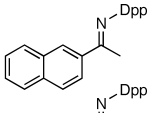	**21a**		**20a**	10	**22aa**	91	7/93	90[h]
2		**21b**		**20a**	10	**22ba**	74	9/91	91
3	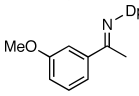	**21c**		**20a**	10	**22ca**	95	11/89	89
4		**21c**		**20a**	5	**22ca**	88	12/88	83
5[d]		**21c**		**20a**	10	**22ca**	71	10/90	94
6[c]	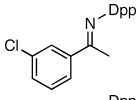	**21d**		**20a**	10	**22da**	84	5/95	77[h]
7	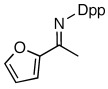	**21e**		**20a**	10	**22ea**	78	6/94	90
8	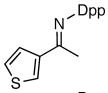	**21f**		**20a**	10	**22fa**	83	3/97	88
9	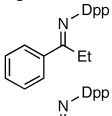	**21g**		**20a**	10	**22ga**	63	8/92	71
10[e]	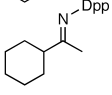	**21h**		**20a**	10	**22ha**	76	<2/98	92
11[e]	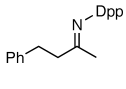	**21i**		**20a**	10	**22ia**	80	4/96	89
12[f]		**21c**		**20b**	10	**22cb**	62[g]	<2/98	90

a) Isolated yield of *E* and *Z* geometrical isomers. *b*) Determined by ^{1}H-NMR analysis of the crude mixture. *c*) (*S*,*S*)-Ph-BPE was used. *d*) 3 eq of **20a** were used. *e*) The reaction was conducted at 0.5 M in THF. $Li(OC_6H_4$-*p*-OMe) was used instead of $Li(OC_6H_4$-*p*-OPh). *f*) Reaction time was 60 h. *g*) Isolated yield after 2 steps (α-addition/isomerization by DBU). *h*) Opposite absolute configuration.

metric addition to a ketone *in situ* provides a more advanced strategy in terms of atom economy.[148—153] Until recently, HCN was the only pronucleophile that met this criterion,[154—156] most likely because deprotonative activation of pronucleophiles to generate a highly active nucleophile requires harsh Brønsted basic conditions, which compromise the catalytic turnover and induce undesirable side reactions. In this context, we envisioned that the allyl cyanide **20a**, which is chemoselectively activated through a soft Lewis acid/hard Brønsted base cooperative catalysis under mild conditions, would serve as an ideal pronucleophile with minimum steric bias to achieve the direct catalytic asymmetric addition to ketone **23** to afford enantioenriched tertiary alcohols under proton transfer conditions. The soft Lewis acid/hard Brønsted base cooperative catalytic system devised for the direct addition of **20a** to ketoimines was applied to the reaction with ketone **23**. A similar set of cooperative catalysts promoted the deprotonation of **20a**, and the addition of *in situ*-generated active nucleophiles to ketones in a γ-fashion and afforded tertiary alcohols **24** bearing a characteristic *Z*-configured olefin with high enantioselectivity (Chart 16).[157] A series of control experiments and kinetic studies suggested that the cationic [Cu/(*R*,*R*)-Ph-BPE]ClO_4 complex and lithium aryloxide were in equilibrium with another state, Cu(OAr)/(*R*,*R*)-Ph-BPE and $LiClO_4$. The former state was the catalytically active species (Chart 17). To further increase the catalytic efficiency based on the mechanistic details, we focused on the enhancement of the Brønsted basicity of lithium aryloxide to facilitate the deprotonation of **20a**, which was revealed to be the rate-determining step in this process. We hypothesized that a hard Lewis basic additive would selectively coordinate to the hard lithium cation through hard–hard interactions and would enhance the Brønsted basicity of the aryloxide.[158—161] Indeed, the addition of triphenylphosphine oxide in equimolar amounts to Li(OC_6H_4-*p*-OMe) substantially facilitated the reaction, allowing the reaction to reach completion at −40 °C with enhanced enantioselectivity. Eventually, the bisphosphine oxide **25** was identified to exhibit even better performance, reducing the required catalytic amount and equivalent of allyl cyanide **20a** to 1 mol% and 2 eq, respectively.[162] With this improved soft Lewis acid/hard Brønsted base/hard Lewis base catalytic system, the direct catalytic asymmetric addition of allyl cyanide **20a** proceeded with a diverse set of non-

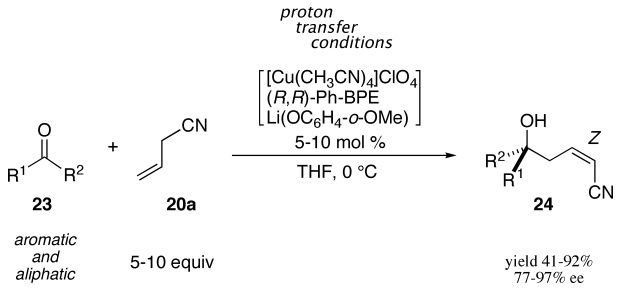

Chart 16. Direct Catalytic Asymmetric Addition of Allyl Cyanide **20a** to Ketones **23**

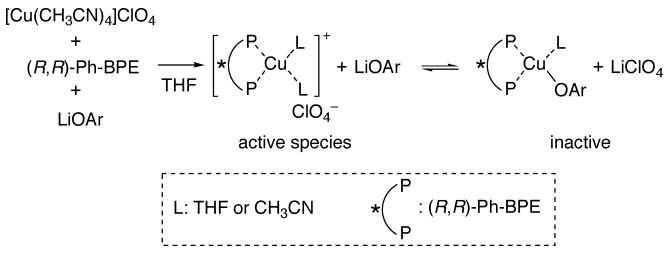

Chart 17. Equilibrium of Cooperative Catalyst Comprised of [$Cu(CH_3CN)_4$]ClO_4, (*R*,*R*)-Ph-BPE, and Lithium Aryloxide

Table 8. Direct Catalytic Asymmetric Addition of Allyl Cyanide **20a** to Ketones **23** Promoted by a Soft Lewis Acid/Hard Brønsted Base/Hard Lewis Base Cooperative Catalyst

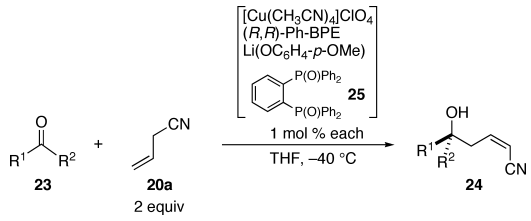

Entry	Ketone		Cat. (mol%)	Time (h)	Yield[a] (%)	ee (%)
1	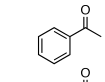	**23a**	1	40	86	99
2			0.5	72	74	99
3	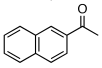	**23b**	1	40	81	98
4	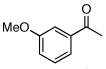	**23c**	1	40	85	98
5		**23d**	1	40	90	99
6		**23e**	1	40	71	99
7		**23f**	2	40	66	99
8		**23g**	1	40	68	91
9		**23h**	1	40	72	99
10		**23i**	1	40	62	88
11[b]		**23j**	5	40	42	>99
12[b]		**23k**	5	72	48	>99
13[b]		**23l**	5	72	88	97
14[b]		**23m**	1	72	53	98
15[b]		**23n**	1	72	67	94
16[b]		**23o**	1	72	68	96
17[b]		**23p**	1	72	67	96
18		**23q**	5	72	55	95
19[b]		**23r**	5	72	39	52

a) Isolated yield. *b*) LiO^{t}Bu was used instead of Li(OC_6H_4-*p*-OMe).

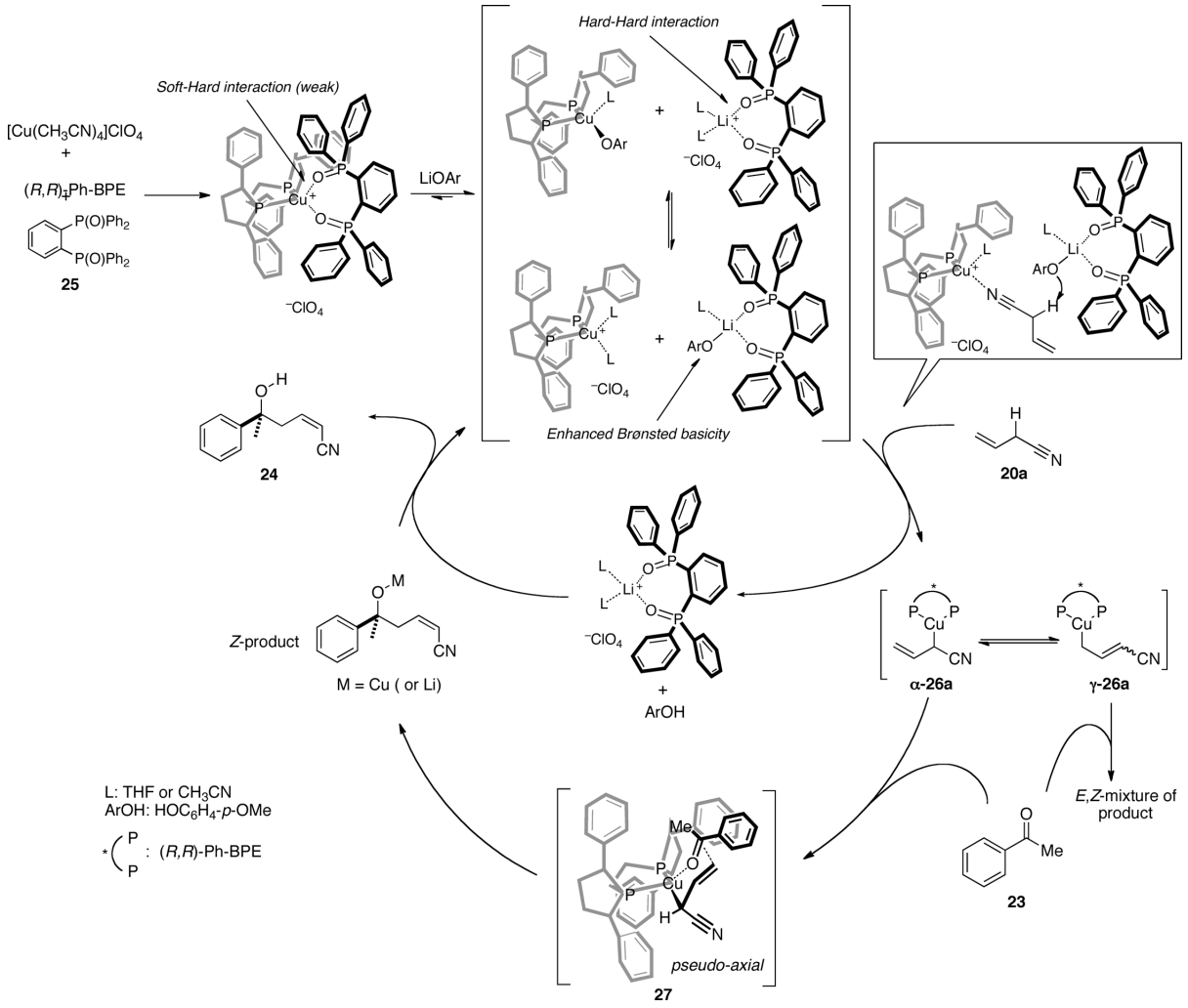

Fig. 5. Proposed Catalytic Cycle, Where a Soft Lewis Acid/Hard Brønsted Base/Hard Lewis Base Catalyst Works Cooperatively

activated ketones **23**, as summarized in Table 8.[163] The nitrile functionality of the product **24** was successfully transformed into amide, aldehyde, and amine functionalities while preserving the *Z*-configuration.

Comprehensive ^{31}P-NMR studies have indicated that **25** is coordinated to a lithium cation, and a plausible catalytic cycle is illustrated in Fig. 5. Mixing $[Cu(CH_3CN)_4]ClO_4$, (*R*,*R*)-Ph-BPE, and **25** generated a cationic complex [Cu/(*R*,*R*)-Ph-BPE/**25**]ClO_4, and the subsequent addition of Li(OC_6H_4-*p*-OMe) led to an equilibrium between {Cu(OC_6H_4-*p*-OMe)/(*R*,*R*)-Ph-BPE+$LiClO_4$/**25**} and {[Cu/(*R*,*R*)-Ph-BPE]ClO_4+Li(OC_6H_4-*p*-OMe)/**25**}. [Cu/(*R*,*R*)-Ph-BPE]ClO_4 activated the allyl cyanide **20a** as a soft Lewis acid, while Li(OC_6H_4-*p*-OMe)/**25** served as a hard Brønsted base to deprotonate **20a**, generating the α-*C*-copper active nucleophile α-**26a**, where the hard Lewis base **25** enhanced the basicity of Li(OC_6H_4-*p*-OMe) through coordination to the Li cations. The substantial acceleration of this step in the presence of **25** would be the basis for the significant improvement in the reaction efficiency: 1 mol% of catalyst loading and 2 eq of **20a**. The initially formed α-**26a** would interconvert to the γ-*C*-copper nucleophile γ-**26a**, which should provide an *E*,*Z* mixture of the γ-addition product **24** following 1,2-addition to the ketones. The exclusive formation of a *Z*-configured olefin would be indicative of the involvement of a six-membered cyclic transition state. The proposed transition state model **27**, in which the reaction proceeds through an α-**26a** intermediate with the nitrile group occupying the pseudoaxial position to avoid steric repulsion with the phenyl group of the (*R*,*R*)-Ph-BPE, explains the origin of the observed *Z*-configuration of the product. The linear relationship between the enantiopurity of Ph-BPE and the enantioselectivity of the product is consistent with the assumption that the monomeric Cu complex is involved in the enantiodiscrimination step.

2.2. Thioamides as Pronucleophiles In the previous section, the development of a soft Lewis acid/hard Brønsted base cooperative catalyst specifically for the chemoselective activation of allylic cyanide pronucleophiles was discussed. The key issue that we focused on was the soft Lewis basicity of the nitrile functionality, which is targeted by a soft Lewis acid to trigger the desired reaction. We envisioned that this strategy would work for other soft Lewis basic pronucleophiles in a similar fashion, allowing for the catalytic deprotonative activation of otherwise low-reactive pronucleophiles. In this context, we focused on the thioamide functionality as a soft Lewis basic variant of carbonyl-type pronucleophiles in the carboxylic acid oxidation state (Chart 18). Thioamides

are widely utilized as useful precursors for the synthesis of a broad range of heterocyclic compounds by exploiting their ambident nucleophilic character at both the sulfur and nitrogen atoms.[164] However, they are rarely recognized as carbon pronucleophiles in enantioselective carbon–carbon bond-forming reactions. Although there have been sporadic studies using thioamide as nucleophiles with the aid of stoichiometric amounts of reagents, there have been no reports on the catalytic generation of active carbon nucleophiles from thioamides and their integration into enantioselective carbon–carbon bond-forming processes.[165—169] Such an approach would be more advantageous than the preceding stoichiometric reactions in terms of atom economy.[12] The following sections will introduce the catalytic activation of thioamide pronucleophiles **28** by a soft Lewis acid/hard Brønsted base cooperative catalytic system to generate thioamide enolates, which was integrated into a subsequent addition to Dpp aldimines **29** and aldehydes **8**, leading to direct catalytic asymmetric Mannich-type and aldol reactions.

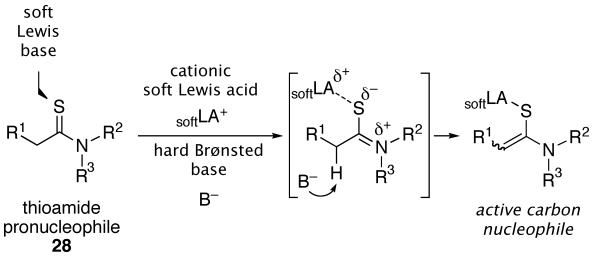

Chart 18. Catalytic Generation of Thioamide Enolate by a Soft Lewis Acid/Hard Brønsted Base Cooperative Catalyst

2.2.1. Direct Catalytic Asymmetric Mannich-Type Reaction of Thioamides Direct catalytic asymmetric Mannich-type reactions have attracted much attention as a useful

Table 9. Direct Catalytic Asymmetric Mannich-Type Reaction of Thioamide **28** Promoted by a Soft Lewis Acid/Hard Brønsted Base Cooperative Catalyst

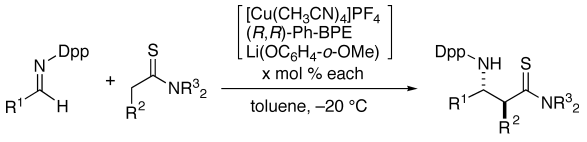

Entry	Imine R[1]		Thioamide		x	Product	Temp. (°C)	Time (h)	Yield[a] (%)	*anti*/*syn*[b]	ee (%)
1		**29a**		**28a**	3	**30aa**	−20	20	95	—	97
2		**29a**		**28a**	1	**30aa**	−20	72	99	—	95
3		**29b**		**28a**	3	**30ba**	−20	48	88	—	95
4		**29c**		**28a**	3	**30ca**	−20	20	96	—	84
5		**29d**		**28a**	3	**30da**	−20	20	94	—	95
6		**29e**		**28a**	3	**30ea**	−20	48	89	—	95
7		**29f**		**28a**	3	**30fa**	−20	48	95	—	93
8		**29g**		**28a**	3	**30ga**	−20	48	90	—	90
9		**29h**		**28a**	3	**30ha**	−20	48	54	—	88
10		**29i**		**28a**	3	**30ia**	−20	48	60	—	78
11		**29j**		**28a**	3	**30ja**	−20	48	66	—	81
12		**29a**		**28b**	3	**30ab**	−20	48	99	—	94
13[c,d]		**29a**		**28c**	10	**30ac**	−20	72	57	89/11	88[c]
14[c,d]		**29a**		**28c**	10	**30ac**	0	72	89	90/10	74[c]
15[c,d]		**29a**	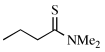	**28d**	10	**30ad**	0	72	84	90/10	53[c]
16[c,d]		**29d**		**28c**	10	**30ac**	0	42	89	89/11	71[c]

a) Yield of isolated product. *b*) Determined by ^{1}H-NMR analysis. *c*) Li(OC$_6$H$_4$-*p*-OMe) was used instead of Li(OC$_6$H$_4$-*o*-OMe). *d*) THF was used as the solvent. *e*) Enantioselectivity of the *anti* diastereomer.

protocol to provide optically active β-amino carbonyl units under proton transfer conditions.[71,72] Recent advances in this methodology have implemented various pronucleophiles in this efficient process, but those in the carboxylic acid oxidation state have yet to be exploited because of the intrinsic difficulty of deprotonative activation. We set out to evaluate a soft Lewis acid/hard Brønsted base cooperative catalytic system for the activation of the thioamide pronucleophile **28** with Dpp aldimines as electrophiles to develop catalytic asymmetric Mannich-type reactions (Chart 19). The reaction of *N*,*N*-diallylthioacetamide **28a** as a commercially available thioamide pronucleophile and imine **29a** was promoted by a slightly modified cooperative catalyst comprised of $[Cu(CH_3CN)_4]PF_6$, (*R*,*R*)-Ph-BPE, and $Li(OC_6H_4$-*o*-OMe) in toluene, affording the corresponding Mannich product **30aa** in 97% ee.[170] The effectiveness of this catalytic system for the catalytic generation of thioamide enolates and the control of the stereochemical course were verified by the broad substrate scope shown in Table 9. A β-elimination of the *N*-Dpp group occurred occasionally at 0 °C, which was circumvented by lowering the reaction temperature to −20 °C. The reaction of an acetyl-type thioamide reached completion with as little as 1—3 mol% of catalyst (Table 9, entries 1—12). The reaction using thioamides **28c** and **28d** derived from propionic or butyric acid was sluggish, and required $Li(OC_6H_4$-*p*-OMe) as a stronger base to afford the product with high *anti*-diastereoselectivity and moderate to good ee (Table 9, entries 13—16).

2.2.2. Direct Catalytic Asymmetric Aldol Reaction of Thioamides The aldol reaction is one of the most fundamental and ubiquitous carbon–carbon bond-forming reactions in both bioorganic transformations and target-oriented organic synthesis.[171,172] Owing to the extensive demand for enantioenriched β-hydroxy carbonyl units produced *via* enantioselective aldol reactions, the asymmetric aldol reaction has been the subject of intense research.[173,174] Although a number of methodologies using preactivated enolates have been developed for catalytic asymmetric aldol reactions, a direct catalytic asymmetric aldol reaction, in which an active enolate is generated in a catalytic manner *via* proton transfer and coupled with subsequent asymmetric addition to an aldehyde, is attracting increasing attention as a more atom-economical[12] and environmentally benign synthetic methodology.[175] The key issue of a direct aldol reaction is the *in situ* catalytic generation of active enolates. Thus the aldol donors implemented in a direct aldol reaction have been largely limited to ketones and aldehydes,[176—183] in which the acidity of the α-proton is sufficiently high for the catalytic generation of the corresponding enolates. For further elaboration of synthetically versatile aldol products, a direct aldol reaction using aldol donors in the carboxylic acid oxidation state providing β-hydroxy carboxylates is more desirable, as it offers a broader functional group manipulation.[184—186] We turned our attention to thioamides, which are in the carboxylic acid oxidation state and are efficiently activated by a soft Lewis acid/hard Brønsted base cooperative catalytic system, as potential aldol donors to achieve a practical direct catalytic aldol reaction under proton transfer conditions (Chart 20).

A model reaction is the reaction of isobutyraldehyde **8n** and *N*,*N*-diallylthioacetamide **28a** in THF at −20 °C in the presence of 10 mol% of an (*R*,*R*)-Ph-BPE/$[Cu(CH_3CN)_4]PF_6$/$Li(OC_6H_4$-*o*-OMe) catalyst, which is effective for direct

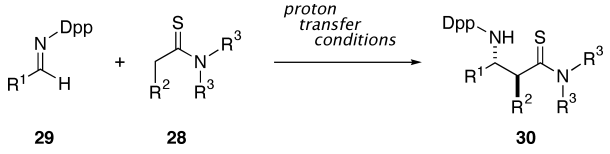

Chart 19. Direct Catalytic Asymmetric Mannich-Type Reaction of Thioamides

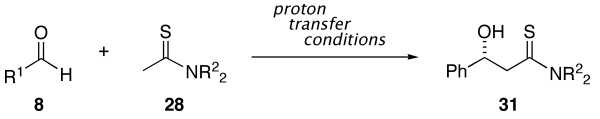

Chart 20. Direct Catalytic Asymmetric Aldol Reaction of Thioamides

Table 10. Direct Catalytic Asymmetric Aldol Reaction of Thioamide **28** Promoted by a Soft Lewis Acid/Hard Brønsted Base Cooperative Catalyst

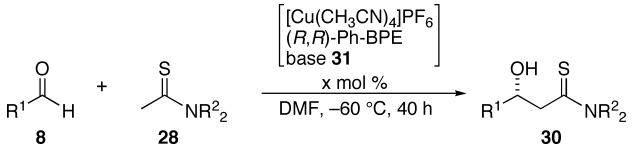

Entry	*x*	Aldehyde R^1CHO		Thioamide R^2=		Product	Yield[a] (%)	ee (%)
1	3	^{i}PrCHO	**8n**	Allyl	**28a**	**30na**	87	91
2	3	^{i}PrCHO	**8n**	Me	**28e**	**30ne**	76	94
3	3	^{c}C$_6$H$_{11}$CHO	**8m**	Allyl	**28a**	**30ma**	98	92
4	3	^{t}BuCHO	**8o**	Allyl	**28a**	**30oa**	90	92
5	9	BnO, CHO	**8p**	Me	**28e**	**30pe**	84	84
6	3	$CH_3(CH_2)_6CHO$	**8q**	Allyl	**28a**	**30qa**	80	89
7	3	$(^cC_6H_{11})CH_2CHO$	**8r**	Allyl	**28a**	**30ra**	81	90
8	3	$(CH_3)_2CHCH_2CHO$	**8s**	Allyl	**28a**	**30sa**	90	90
9	3	$PhCH_2CH_2CHO$	**8k**	Allyl	**28a**	**30ka**	63	88
10	3	$BzO(CH_2)_6CHO$	**8t**	Allyl	**28a**	**30ta**	82	90

Base **31**: 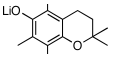

a) Isolated yield.

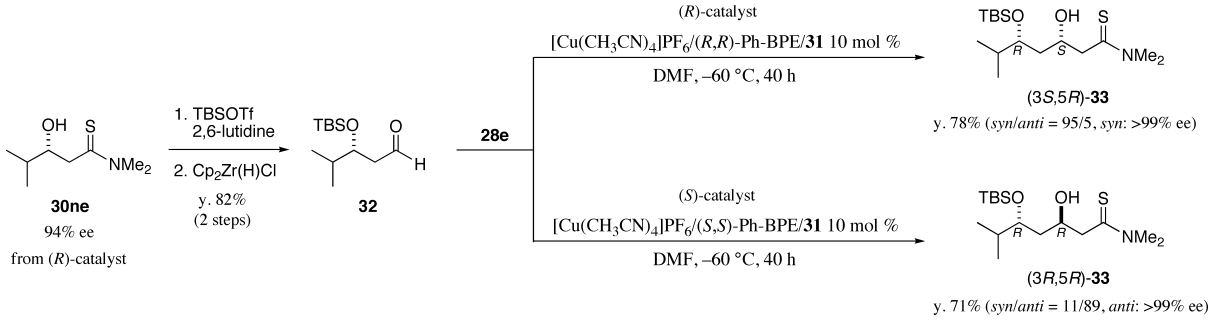

Chart 21. Stereoselective Synthesis of *anti*- and *syn*-Diols *via* a Direct Catalytic Asymmetric Aldol Reaction of Thioamides

Table 11. Direct Catalytic Asymmetric Aldol Reaction of Thioamide **28a** and Aromatic Aldehydes Promoted by a Soft Lewis Acid/Hard Brønsted Base Cooperative Catalyst

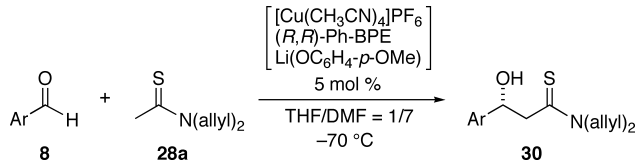

Entry	Aldehyde	Ar	Product	Time (h)	Yield[a] (%)	ee (%)
1	Ph	**8a**	**30aa**	20	94 (1.7)	79
2	2-Naph	**8u**	**30ua**	20	96 (3.0)	79
3	2-MeC_6H_4	**8v**	**30va**	40	89 (3.6)	67
4	4-MeC_6H_4	**8w**	**30wa**	20	88 (2.1)	79
5	3-$MeOC_6H_4$	**8x**	**30xa**	40	85 (3.4)	82
6	4-FC_6H_4	**8e**	**30ea**	40	96 (3.0)	74
7	4-ClC_6H_4	**8y**	**30ya**	40	80 (2.2)	71
8	2-Thienyl	**8z**	**30za**	40	74 (ND[d])	91

a) Isolated yield. Yield of dehydrated product is provided in parentheses (determined by ^{1}H-NMR of the crude mixture). *b*) Not detected.

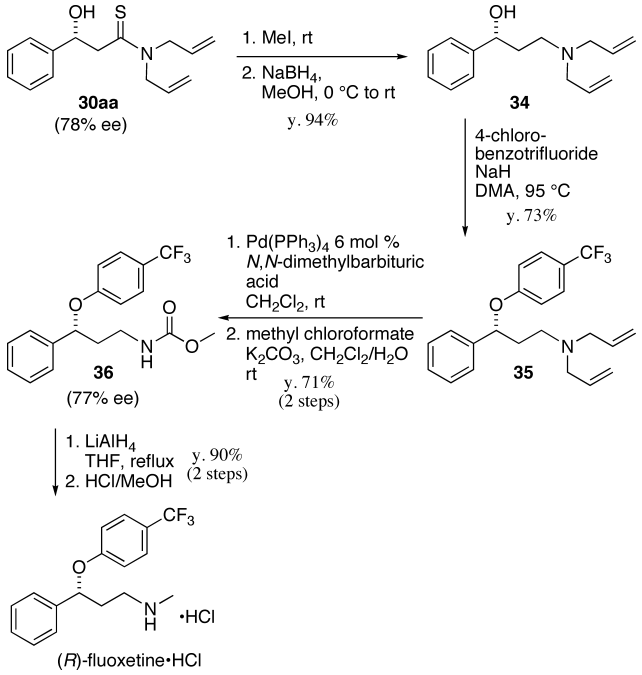

Chart 22. Concise Enantioselective Synthesis of (*R*)-Fluoxetine *via* a Direct Catalytic Asymmetric Aldol Reaction of Thioamide

Mannich-type reactions of thioamides,[170] but it resulted in unexpectedly poor conversion. Spectroscopic analysis revealed that the catalytic cycle was arrested by product inhibition, which was successfully avoided using the Lewis basic *N*,*N*-dimethylformamide (DMF) as solvent. The reaction conditions were further optimized with the use of the stronger Brønsted base 2,2,5,7,8-pentamethylchromanol lithium salt **31** at −60 °C, which exhibited the best performance in promoting a direct aldol reaction without any undesirable dehydration reaction to give α,β-unsaturated thioamides. The scope of the present aldol reaction is summarized in Table 10.[187] Branched aldehydes **8m**, **8o**, and **8p** other than isobutyraldehyde **8n** are well suited for the present catalytic system, and exhibit high enantioselectivity (Table 10, entries 1—5). Of particular note is the compatibility of the nonbranched aldehydes **8k** and **8q**—**t**, which are susceptible to self-condensation under basic conditions. They afforded the desired products without the formation of self-aldol products (Table 10, Entries 6—10). An ester functionality was also tolerated in the reaction of **8t**, confirming the mild basic conditions (Table 10, entry 10). The aldol products derived from aromatic aldehydes were more prone to dehydration. The use of the milder base Li(OC_6H_4-*p*-OMe) at a lower reaction temperature (−70 °C) in a binary solvent system (THF/DMF=1/7) circumvented the formation of α,β-unsaturated thioamides, whereas the enantioselectivity was moderate partially due to the retro-aldol reaction (Table 11).[188]

The synthetic utility of the present protocol was highlighted in its application to stereoselective 1,3-diol synthesis (Chart 21). A two-step sequence of TBS protection followed by reduction of the thioamide functionality with a Schwartz reagent converted **30ne** to aldehyde **32** in 82% yield,[189] which was then subjected to a second direct aldol reaction with either an (*R*)- or (*S*)-catalyst. The reaction proceeded stereoselectively to afford diols (3*S*,5*R*)-**33** and (3*R*,5*R*)-**33**, respectively, indicating that the catalyst mainly controlled the newly formed stereogenic center. Facile manipulation of the thioamide functionality of the aldol product **30aa** enabled a concise asymmetric synthesis of (*R*)-fluoxetine (Chart 22).[190—192] Desulfurization of **3aa** was conducted through a two-step sequence of the activation of thioamide with MeI and a subsequent hydride reduction with $NaBH_4$,[193] affording the corresponding diallylamine **34** in 94% yield. Installation of the requisite 4-trifluoromethylphenyl group under basic conditions gave aryl ether **35**.[194,195] A palladium-catalyzed deallylation protocol with a following carbamate formation afforded **36** in 71% yield in two steps.[196] Reduction of **37** with $LiAlH_4$ and subsequent treatment with

HCl/MeOH delivered (*R*)-fluoxetine · HCl.

Conclusion

Two distinct sets of catalyst, an RE metal/amide-based ligand catalyst and a soft Lewis acid/hard Brønsted base catalyst, were effective in promoting a series of catalytic asymmetric reactions under proton transfer conditions, driven by cooperative catalysis where both reaction partners were activated in concert. The cooperative activation enabled the construction of tetrasubstituted stereogenic centers using nonactivated substrates without generating reagent-derived waste. The RE metal/amide-based ligand catalyst was characterized by its unique nature in controlling the stereochemical course through both hydrogen bonds and metal coordination, allowing its use in highly coordinative substrates in asymmetric catalysis. The dynamic nature of the association/dissociation properties between flexible amide-based ligands and RE metals is particularly noteworthy in exhibiting high catalytic performance and allows these compounds to acquire multifunctionality linked to their three-dimensional structure in response to a given chemical trigger. This intrinsic property is closely related to the molecular recognition of the amide-based ligand in high fidelity, and will lead to the design of time- and structure-dependent multifunctional catalysts. The soft Lewis acid/hard Brønsted base catalysts provided a powerful strategy to activate soft Lewis basic pronucleophiles catalytically, such as allylic cyanides and thioamides, under mild basic conditions. By harnessing the soft/hard specificity with this catalytic system, the *in situ* chemoselective generation of active nucleophiles from otherwise low-reactive nucleophiles proceeded smoothly to achieve direct addition of the above pronucleophiles to carbonyl-type electrophiles, including ketoimines and ketones. The utility of these two types of catalyst is expanding, likely leading to the revision of other inefficient transformations with atom-economical reactions under proton transfer conditions.

Acknowledgments I would like to express my sincere gratitude to Prof. Masakatsu Shibasaki at the University of Tokyo (currently Director of the Institute of Microbial Chemistry) for his direction and fruitful suggestions with enormous scientific enthusiasm. I am deeply indebted to a highly talented group of coworkers whose names appear in the reference section of this review, and I thank them for their critical contributions. These works were financially supported by a Grant-in-Aid for Start-up and a Grant-in-Aid for Young Scientists (B) from the Japan Society for the Promotion of Science, and a Grant-in-Aid for Innovative Areas from the Japanese Ministry of Education, Culture, Sports, Science and Technology. In addition, financial support from the Chugai Award in Synthetic Organic Chemistry, Mitsubishi Chemical Corporation Fund, Sankyo Foundation for Life Sciences, and Sumitomo Foundation is gratefully acknowledged. Dr. Motoo Shiro at the Rigaku Corporation is gratefully acknowledged for technical assistance in the X-ray crystallographic analysis of new compounds and complexes.

References and Notes

1) "Comprehensive Asymmetric Catalysis," ed. by Jacobsen E. N., Pfaltz A., Yamamoto H., Springer, Berlin, 1999 and 2003 (for Supplement I).
2) "New Frontiers in Asymmetric Catalysis," ed. by Mikami K., Lautens M., Wiley, Weinheim, 2007.
3) Walsh P. J., Kozlowski M. C., "Fundamentals of Asymmetric Catalysis," University Science Books, California, U.S.A., 2009.
4) For a recent review, see: Kanai M., Kato N., Ichikawa E., Shibasaki, M., *Synlett*, **2005**, 1491—1508 (2005).
5) For a recent review, see: Matsunaga S., Shibasaki M., *Bull. Chem. Soc. Jpn.*, **81**, 60—75 (2008).
6) For a recent review, see: Yamamoto H., Futatsugi K., *Angew. Chem., Int. Ed.*, **44**, 1924—1942 (2005).
7) For a recent review, see: Ma J.-A., Cahard D., *Angew. Chem., Int. Ed.*, **43**, 4566—4583 (2004).
8) "Multimetallic Catalysis in Organic Synthesis," ed. by Shibasaki M., Yamamoto Y., Wiley-VCH, New York, 2004.
9) For a recent review, see: Houk K. N., List B., *Acc. Chem. Res.*, **37**, special issue (2004).
10) For a recent review, see: Paull D. H., Abraham C. J., Screba M. T., Alden-Danforth E., Lectka T., *Acc. Chem. Res.*, **41**, 655—663 (2008).
11) For a recent review, see: Shibasaki M., Kanai M., Matsunaga S., Kumagai N., *Acc. Chem. Res.*, **42**, 1117—1127 (2009).
12) Trost B. M., *Scienece*, **254**, 1471—1477 (1991).
13) Genet J.-P., Greck C., Lavergne D., "Modern Amination Methods," Chap. 3, ed. by Ricci A., Wiley-VCH, Weinheim, 2000, pp. 65—102.
14) Krohn K., "Organic Synthesis Highlights," Wiley-VCH, Weinheim, 1991, pp. 45—53.
15) Huisgen R., Jakob F., *Justus Liebigs Ann. Chem.*, **590**, 37—47 (1954).
16) For electrophilic amination using azodicarboxylates, see: Diels O., *Justus Liebigs Ann. Chem.*, **429**, 1—55 (1922).
17) For electrophilic amination using azodicarboxylates, see: Diels O., Behncke H., *Chem. Ber.*, **57**, 653—656 (1924).
18) Evans D. A., Nelson S. G., *J. Am. Chem. Soc.*, **119**, 6452—6453 (1997).
19) Evans D. A., Johnson D. S., *Org. Lett.*, **1**, 595—598 (1999).
20) For a review of catalytic asymmetric electrophilic amination of carbonyl compounds, see: Duthaler R. O., *Angew. Chem., Int. Ed.*, **42**, 975—978 (2003).
21) For a review of catalytic asymmetric electrophilic amination of carbonyl compounds, see: Greck C., Drouillat B., Thomassigny C., *Eur. J. Org. Chem.*, **2004**, 1377—1385 (2004).
22) For a review of catalytic asymmetric electrophilic amination of carbonyl compounds, see: Janey J. M., *Angew. Chem., Int. Ed.*, **44**, 4292—4300 (2005).
23) For a review of catalytic asymmetric electrophilic amination of carbonyl compounds, see: Cativiela C., Ordóñez M., *Tetrahedron: Asymmetry*, **20**, 1—63 (2009).
24) Negoro T., Murata M., Ueda S., Fujitani B., Ono Y., Kuromiya A., Komiya, M., Suzuki K., Matsumoto J.-I., *J. Med. Chem.*, **41**, 4118—4129 (1998).
25) Kurono M., Fujiwara I., Yoshida K., *Biochemistry*, **40**, 8216—8226 (2001).
26) Giannoukakis N., *Curr. Opin. Invest. Drugs*, **7**, 916—923 (2006).
27) Wang W., Huang Y., Tang N., *Spectrochim. Acta Part A*, **66**, 1058—1062 (2007).
28) For an example of a rare earth metal/amide ligand catalyst in asymmetric catalysis, see: Nishida A., Yamanaka M., Nakagawa M., *Tetrahedron Lett.*, **40**, 1555—1558 (1999).
29) For an example of a rare earth metal/amide ligand catalyst in asymmetric catalysis, see: Sudo Y., Shirasaki D., Harada S., Nishida A., *J. Am. Chem. Soc.*, **130**, 12588—12589 (2008).
30) Mashiko T., Hara K., Tanaka D., Fujiwara Y., Kumagai N., Shibasaki M., *J. Am. Chem. Soc.*, **129**, 11342—11343 (2007).
31) For an alternative enantioselective synthetic approach toward AS-3201 reported after our report, see: Watanabe T., Kawabata T., *Heterocycles*, **76**, 1593—1606 (2008).
32) For an alternative enantioselective synthetic approach toward AS-3201 reported after our report, see: He R., Wang X., Hashimoto T., Maruoka K., *Angew. Chem., Int. Ed.*, **47**, 9466—9468 (2008).
33) For an alternative enantioselective synthetic approach toward AS-3201 reported after our report, see: Trost B. M., Osipov M., Dong G., *Org. Lett.*, **12**, 1276—1279 (2010).
34) "Sigma-Aldrich Handbook of Fine Chemicals 2009—2010," Sigma-Aldrich, Milwaukee, WI, 2008.
35) Furuno H., Hayano T., Kambara T., Sugimoto Y., Hanamoto T., Tanaka Y., Jin Y. Z., Kagawa T., Inanaga J., *Tetrahedron*, **59**, 10509—10523 (2003).
36) Mashiko T., Kumagai N., Shibasaki, M., *Org. Lett.*, **10**, 2725—2728 (2008).
37) Shibasaki, M., Kumagai N., Mashiko T., *Curr. Opin. Drug Discov. Dev.*, **12**, 862—875 (2009).
38) Li S., Wang S., *J. Heterocyclic Chem.*, **45**, 1875—1878 (2008) and references cited therein.
39) Mashiko T., Kumagai N., Shibasaki M., *J. Am. Chem. Soc.*, **131**,

14990—14999 (2009).
40) Henry L., *C. R. Hebd. Seances Acad. Sci.*, **120**, 1265—1268 (1895).
41) For a review, see: Shibasaki M., Gröger H., "Comprehensive Asymmetric Catalysis," Vol. III, ed. by Jacobsen E. N., Pfaltz A., Yamamoto H., Springer, Berlin, 1999, pp. 1075—1090.
42) Boruwa J., Gogoi N., Saikia P. P., Barua N. C., *Tetrahedron: Asymmetry*, **17**, 3315—3326 (2006).
43) Palomo C., Oiarbide M., Laso A., *Eur. J. Org. Chem.*, **2007**, 2561—2574 (2007).
44) Sasai H., Suzuki T., Arai S., Arai T., Shibasaki M., *J. Am. Chem. Soc.*, **114**, 4418—4420 (1992).
45) For *syn*-selective reaction, see: Sasai H., Tokunaga T., Watanabe S., Suzuki T., Itoh N., Shibasaki M., *J. Org. Chem.*, **60**, 7388—7389 (1995).
46) For *syn*-selective reaction, see: Sohtome Y., Takemura N., Takada K., Takagi R., Iguchi T., Nagasawa K., *Chem. Asian J.*, **2**, 1150—1160 (2007) and references cited therein.
47) For *syn*-selective reaction, see: Arai T., Takashita R., Endo Y., Watanabe M., Yanagisawa A., *J. Org. Chem.*, **73**, 4903—4906 (2008) and references cited therein.
48) Uraguchi D., Sakaki S., Ooi T., *J. Am. Chem. Soc.*, **129**, 12392—12393 (2007).
49) Handa S., Nagawa K., Sohtome Y., Matsunaga S., Shibasaki M., *Angew. Chem., Int. Ed.*, **47**, 3230—3233(2008).
50) For a partially successful example after our report, see: Blay G., Hernández-Olmos V., Pedro J. R., *Org. Lett.*, **12**, 3058—3061 (2010).
51) For the *anti*-selective catalytic asymmetric nitroaldol reaction of benzaldehyde using hydroxynitrile lyase, see: Gruber-Khadjawi M., Purkarthofer T., Skranc W., Griengl H., *Adv. Synth. Catal.*, **349**, 1445—1450 (2007).
52) Seebach D., Beck A. K., Mukhopadhyay T., Thomas E., *Helv. Chim. Acta*, **65**, 1101—1133 (1982) and references cited therein.
53) Nitabaru T., Kumagai N., Shibasaki M., *Tetrahedron Lett.*, **49**, 272—276 (2008).
54) In contrast to the possible incomplete complexation with a ligand due to the nonordered aggregation state of $Nd(O^iPr)_3$, reproducible formation of the desired complex was anticipated using μ-oxo isopropoxide $Nd_5O(O^iPr)_{13}$. $Nd_5O(O^iPr)_{13}$ is available from the Kojundo Chemical Co. Ltd., Japan http://www.kojundo.co.jp/English/index.html, fax: +81–49–284–1351, e-mail: sales@kojundo.co.jp.
55) Li C., Ren S.-F., Hou J.-L., Yi H.-P., Zhu S.-Z., Jiang X. K., Li Z.-T., *Angew. Chem., Int. Ed.*, **44**, 5725—5729 (2005).
56) Nitabaru T., Nojiri A., Kobayashi M., Kumagai N., Shibasaki M., *J. Am. Chem. Soc.*, **131**, 13860—13869 (2009).
57) Tanaka N., Tamai T., Mukaiyama H., Hirabayashi A., Muranaka H., Ishikawa T., Kobayashi J., Akahane S., Akahane M., *J. Med. Chem.*, **46**, 105—112 (2003) and references cited therein.
58) For the first catalytic asymmetric nitro-Mannich-type reaction, see: Yamada K.-I., Harwood S. J., Gröger H., Shibasaki M., *Angew. Chem., Int. Ed.*, **38**, 3504—3506 (1999).
59) For the first enantioselective and diastereoselective catalytic nitro-Mannich reaction, see: Yamada K.-I., Moll G., Shibasaki M., *Synlett*, **2001**, 980—982 (2001).
60) For a review, see: Westermann B., *Angew. Chem., Int. Ed.*, **42**, 151—153 (2003).
61) For a review, see: Marqués-López E., Merino P., Tejero T., Herrera R. P., *Eur. J. Org. Chem.*, **2009**, 2401—2420 (2009).
62) Nitabaru T., Kumagai N., Shibasaki M., *Molecules*, **15**, 1280—1290 (2010).
63) For a recent review, see: Corey E. J., Guzman-Perez A., *Angew. Chem., Int. Ed.*, **37**, 388—401 (1998).
64) For a recent review, see: Christoffers J., Mann A., *Angew. Chem., Int. Ed.*, **40**, 4591—4592 (2001).
65) For a recent review, see: Douglas C. J., Overman L. E., *Proc. Natl. Acad. Sci. U.S.A.*, **101**, 5363—5367 (2004).
66) For a recent review, see: Trost B. M., Jiang C., *Synthesis*, **2006**, 369—396 (2006).
67) For a review on α-cyanocarbanions, see: Arseniyadis S., Kyler K. S., Watt D. S., *Org. React.*, **31**, 1—71 (1984).
68) For a review on α-cyanocarbanions, see: Fleming F. F., Shook B. C., *Tetrahedron*, **58**, 1—23 (2002).
69) For a review on α-cyanocarbanions, see: Fleming F. F., Iyer P. S., *Synthesis*, **2006**, 893—913 (2006).
70) For a recent review on direct Mannich reactions using unmodified pronucleophiles, see: Ting A., Schaus S. E., *Eur. J. Org. Chem.*, **2007**, 5797—5815 (2007) and references cited therein.
71) For a recent review on direct Mannich reactions using unmodified pronucleophiles, see: Verkade J. M. M., van Hemert L. J. C., Quaedflieg P. J. L. M., Rutjes F. P. J. T., *Chem. Soc. Rev.*, **37**, 29—41 (2008).
72) For a general review on catalytic asymmetric Mannich reactions, see: Kobayashi S., Ueno M., "Comprehensive Asymmetric Catalysis," Supplement 1, Chapter 29.5, ed. by Jacobsen E. N., Pfaltz A., Yamamoto H., Springer, Berlin, 2003, p. 143.
73) For a general review on catalytic asymmetric Mannich reactions, see: Friestad G., Mathies A. K., *Tetrahedron*, **63**, 2541—2569 (2007).
74) Marigo M., Kjærsgaard A., Juhl K., Gathergood N., Jørgensen K. A., *Chem. Eur. J.*, **9**, 2359—2367 (2003).
75) Hamashima Y., Sasamoto N., Hotta D., Somei H., Umebayashi N., Sodeoka M., *Angew. Chem., Int. Ed.*, **44**, 1525—1529 (2005).
76) Ting A., Lou S., Schaus S. E., *Org. Lett.*, **8**, 2003—2006 (2006).
77) Tillman A. L., Ye J., Dixon D. J., *Chem. Commun.*, **2006**, 1191—1193 (2006).
78) Yamaoka Y., Miyabe H., Yoshizumi Y., Takemoto Y., *Synthesis*, **2007**, 2571—2575 (2007).
79) Chen Z., Morimoto H., Matsunaga S., Shibasaki M., *J. Am. Chem. Soc.*, **130**, 2170—2171 (2008).
80) Nojiri A., Kumagai N., Shibasaki M., *J. Am. Chem. Soc.*, **130**, 5630—5631 (2008).
81) For a representative example of a Mannich-type reaction of 1,3-dicarbonyl compounds generating quaternary stereocenters displaying both *syn*- and *anti*-diastereoselectivity reported after our report, see: Hatano M., Horibe T., Ishihara K., *J. Am. Chem. Soc.*, **132**, 56—57 (2010).
82) For a representative example of a Mannich-type reaction of α-cyanoketones generating quaternary stereocenters reported after our report, see: Lee J. H., Kim D. Y., *Adv. Synth. Catal.*, **351**, 1779—1782(2009).
83) Nojiri A., Kumagai N., Shibasaki M., *J. Am. Chem. Soc.*, **131**, 3779—3784 (2009).
84) For a general review on enantioselectivity reversal using a single chiral source, see: Tanaka T., Hayashi, M., *Synthesis*, **2008**, 3361—3376(2008) and references therein.
85) For a notable example of an asymmetric catalyst exhibiting a sharp enantio-switching depending on the assembly state of the catalyst, see: Kato N., Mita T., Kanai M., Therrien B., Kawano M., Yamaguchi K., Danjo H., Sei Y., Sato A., Furusho S., Shibasaki M., *J. Am. Chem. Soc.*, **128**, 6768—6769 (2006).
86) For an example of asymmetric catalysts with an induced-fit mechanism, see: Kawabata T., Nagato M., Takasu, K., Fuji K., *J. Am. Chem. Soc.*, **119**, 3169—3170 (1997).
87) For a review on asymmetric activation and deactivation, see: Mikami K., Aikawa K., "New Frontier in Asymmetric Catalysis," ed. by Mikami K., Lautens M., Wiley, New York, 2007, pp. 221—257.
88) For an example of an artificial allosteric catalyst, see: Gianneschi N. C., Bertin P. A., Nguyen S. T., Mirkin C. A., Zakharov L. N., Rheingold A. L., *J. Am. Chem. Soc.*, **125**, 10508—10509 (2003).
89) For an example of a photoswitchable achiral catalyst achieving an ON state and an OFF state, see: Stoll R. S., Peters M. V., Kuhn A., Heiles S., Goddard R., Bühl M., Thiele C. M., Hecht S., *J. Am. Chem. Soc.*, **131**, 357—367 (2009).
90) For a leading example of a conformationally dynamic metal-based asymmetric catalyst in which the conformational chirality was dynamically transferred to the catalytic center, see: Yu J., RajanBabu T. V., Parquette J. R., *J. Am. Chem. Soc.*, **130**, 7845—7846 (2008).
91) Ptashne M., Gann A., *Curr. Biol.*, **8**, R812—R822 (1998).
92) Harrison S. C., *Nature Struct. Mol. Biol.*, **11**, 12—15 (2004).
93) Heilmann I., Pidkowich M. S., Girke T., Shanklin J., *Proc. Natl. Acad. Sci. U.S.A.*, **101**, 10266—10271 (2004).
94) For a general review of catalytic asymmetric conjugate addition, see: Krause N., Hoffmann-Röder A., *Synthesis*, **2001**, 171—196 (2001).
95) For a general review of catalytic asymmetric conjugate addition, see: Sibi M. P., Manyem S., *Tetrahedron*, **56**, 8033—8061 (2000).
96) For a general review of catalytic asymmetric conjugate addition, see: Alexakis A., Benhaim C., *Eur. J. Org. Chem.*, **2002**, 3221—3236 (2002).
97) For a general review of catalytic asymmetric conjugate addition, see: Christoffers J., Baro A., *Angew. Chem., Int. Ed.*, **42**, 1688—1690 (2003).

98) For a general review of catalytic asymmetric conjugate addition, see: Tsogoeva S. B., *Eur. J. Org. Chem*., **2007**, 1701—1716 (2007).
99) Kawato Y., Takahashi N., Kumagai N., Shibasaki M., *Org. Lett.*, **12**, 1484—1487 (2010).
100) For a review, see: Philip D., Stoddart J. F., *Angew. Chem., Int. Ed.*, **35**, 1155—1196 (1996).
101) For a review, see: Leininger S., Olenyuk B., Stang P. J., *Chem. Rev.*, **100**, 853—907 (2000).
102) For a review, see: Fraser H., Craig S. L., Nuckolls C., Rebek J. Jr., *Angew. Chem., Int. Ed.*, **114**, 1556—1557 (2002).
103) For a review, see: Fujita M., Tominaga M., Hori A., Therrien B., *Acc. Chem. Res.*, **38**, 371—380 (2005).
104) For a review, see: Lehn J.-M., *Chem. Soc. Rev.*, **36**, 151—160 (2007).
105) Matsuzawa A., Nojiri A., Kumaagi N., Shibasaki M., *Chem. Eur. J.*, **16**, 5036—5042 (2010).
106) Eliel S., Wilen S. H., Mander L. N., "Stereochemistry of Organic Compounds," Wiley & Sons, New York, 1994.
107) Jacques J., Collet, A., Wilen S. H., "Enantiomers, Racemates, and Resolutions," Krieger Publishing, Malabar, 1994.
108) For an example of similar experiments, see: Klussmann M., White A. J. P., Armstrong A., Blackmond D. G., *Angew. Chem., Int. Ed.*, **45**, 7985—7989 (2006).
109) Hayashi Y., Matsuzawa M., Yamaguchi J., Yonehara S., Matsumoto Y., Shoji M., Hashizume D., Koshino H., *Angew. Chem., Int. Ed.*, **45**, 4593—4597 (2006).
110) "Modern Aldol Reactions," ed. by Mahrwald R., Wiley-VCH, Weinheim, 2004.
111) For a recent review, see: Shibasaki M., Yoshikawa N., *Chem. Rev.*, **102**, 2187—2209 (2002).
112) For a recent review, see: Alcaide B., Almendros P., *Eur. J. Org. Chem.*, **2002**, 1595—1601 (2002).
113) For a recent review, see: Saito S., Yamamoto H., *Acc. Chem. Res.*, **37**, 570—579 (2004).
114) For a recent review, see: Notz W., Tanaka F., Barbas C. F. III, *Acc. Chem. Res.*, **37**, 580—591 (2004).
115) For a recent review, see: Córdova A., *Acc. Chem. Res.*, **37**, 102—112 (2004).
116) For a recent review, see: Marques M. M. B., *Angew. Chem., Int. Ed.*, **45**, 348—352 (2006).
117) For a recent review, see: Guillena G., Nájera C., Ramón D. J., *Tetrahedron: Asymmetry*, **18**, 2249—2293 (2007).
118) For a recent review, see: Mukherjee S., Yang J. W., Hoffmann S., List B., *Chem. Rev.*, **107**, 5471—5569 (2007).
119) For *N*-acylthiazolidinethiones, see: Evans D. A., Downey C. W., Hubbs J. L., *J. Am. Chem. Soc.*, **125**, 8706—8707 (2003).
120) For malonic acid half-thioesters, see: Magdziak D., Lalic G., Lee H. M., Fortner K. C., Aloise A. D., Shair M. D., *J. Am. Chem. Soc.*, **127**, 7284—7285 (2005).
121) For *N*-acyl pyrroles, see: Harada S., Handa S., Matsunaga S., Shibasaki M., *Angew. Chem., Int. Ed.*, **44**, 4365—4368 (2005).
122) For trichloromethyl ketones, see: Morimoto H., Wiedemann S. H., Yamaguchi A., Harada S., Chen Z., Matsunaga S., Shibasaki M., *Angew. Chem., Int. Ed.*, **45**, 3146—3150 (2006).
123) For *N*-acyl Boc-amides, see: Saito S., Kobayashi S., *J. Am. Chem. Soc.*, **128**, 8704—8705 (2006).
124) Bordwell F. G., *Acc. Chem. Res.*, **21**, 456—463 (1988).
125) Richard J. P., Williams G., Gao J., *J. Am. Chem. Soc.*, **121**, 715—726 (1999).
126) For an example of catalytic chemoselective nucleophilic activation of alkylnitrile, see: Kumagai N., Matsunaga M., Shibasaki M., *J. Am. Chem. Soc.*, **126**, 13632—13633 (2004).
127) For an example of catalytic chemoselective nucleophilic activation of alkylnitrile, see: Kumagai N., Matsunaga S., Shibasaki M., *Chem. Commun.*, **2005**, 3600—3602 (2005).
128) For an example of catalytic chemoselective nucleophilic activation of alkylnitrile, see: Fan L., Ozerov O. V., *Chem. Commun.*, **2005**, 4450—4452 (2005).
129) For an example of catalytic chemoselective nucleophilic activation of alkylnitrile, see: Kumagai N., Matsunaga S., Shibasaki M., *Tetrahedron*, **63**, 8598—8608 (2007).
130) For an example of catalytic chemoselective nucleophilic activation of alkylnitrile, see: Goto A., Endo K., Ukai Y., Irle S., Saito S., *Chem. Commun.*, **2008**, 2212—2214 (2008).
131) For an example of the use of allylic cyanides as pronucleophiles in racemic reactions, see: Kisanga P. B., Verkade J. G., *J. Org. Chem.*, **67**, 426—430 (2002).
132) For an example of the use of allylic cyanides as pronucleophiles in racemic reactions, see: Aydin J., Szabó K. J., *Org. Lett.*, **10**, 2881—2884 (2008).
133) For an example of the use of allylic cyanides as pronucleophiles in racemic reactions, see: Swartz B. D., Reinartz N. M., Brennessel W. W., García J. J., Jones W. D., *J. Am. Chem. Soc.*, **130**, 8548—8554 (2008).
134) For a review of the electrophilic activation of nitrile functionality through soft Lewis acids, see: Michelin R. A., Mozzon M., Bertani R., *Coord. Chem. Rev.*, **147**, 299—338 (1996).
135) For a review of the electrophilic activation of nitrile functionality through soft Lewis acids, see: Kukushkin V. Y., Pombeiro A. J. L., *Chem. Rev.*, **102**, 1771—1802 (2002).
136) Calculated at the B3LYP/6-31G+(d,p) level in ref. 142.
137) Vachal P., Jacobsen E. N., *Org. Lett.*, **2**, 867—870 (2000).
138) Vachal P., Jacobsen E. N., *J. Am. Chem. Soc.*, **124**, 10012—10014 (2002).
139) Rueping M., Sugiono E., Moreth S. A., *Adv. Synth. Catal.*, **349**, 759—764 (2007).
140) Zhuang W., Saaby S., Jørgensen K. A., *Angew. Chem., Int. Ed.*, **43**, 4476—4478 (2004).
141) For a review, see: Weinreb S. M., Orr R. K., *Synthesis*, **2005**, 1205—1227 (2005).
142) Yazaki R., Nitabaru T., Kumagai N., Shibasaki M., *J. Am. Chem. Soc.*, **130**, 14477—14478 (2008).
143) For a recent review of catalytic asymmetric synthesis of tertiary alcohols, see: Riant O., Hannedouche J., *Org. Biomol. Chem.*, **5**, 873—888 (2007).
144) For a recent review of catalytic asymmetric synthesis of tertiary alcohols, see: Shibasaki M., Kanai M., *Chem. Rev.*, **108**, 2853—2873 (2008).
145) For a recent review of catalytic asymmetric synthesis of tertiary alcohols, see: Hatano M., Ishihara K., *Synthesis*, **2008**, 1647—1675 (2008).
146) For a recent review of catalytic asymmetric synthesis of tertiary alcohols, see: Trost B. M., Weiss A. H., *Adv. Synth. Catal.*, **351**, 963—983 (2009).
147) For a recent review of catalytic asymmetric synthesis of tertiary alcohols, see: Adachi S., Harada T., *Eur. J. Org. Chem.*, **2009**, 3661—3671 (2009).
148) For an example of catalytic asymmetric addition to ketones coupled with hydrogenation, see: Lam H. W., Joensuu P. M., *Org. Lett.*, **7**, 4225—4228 (2005).
149) For an example of catalytic asymmetric addition to ketones coupled with hydrogenation, see: Kong J.-R., Ngai M.-Y., Krische M. J., *J. Am. Chem. Soc.*, **128**, 718—719 (2006).
150) For an example of catalytic asymmetric addition to ketones coupled with hydrogenation, see: Deschamp J., Chuzel O., Hannedouche J., Riant O., *Angew. Chem., Int. Ed.*, **45**, 1292—1297 (2006).
151) For an example of catalytic asymmetric addition to ketones coupled with hydrogenation, see: Komanduri V., Krische M. J., *J. Am. Chem. Soc.*, **128**, 16448—16449 (2006).
152) For an example of catalytic asymmetric addition to ketones coupled with hydrogenation, see: Shiomi T., Nishiyama H., *Org. Lett.*, **9**, 1651—1654 (2007).
153) For an example of catalytic asymmetric addition to ketones coupled with hydrogenation, see: Bower J. F., Kim I. S., Patman R. L., Krische M. J., *Angew. Chem., Int. Ed.*, **48**, 34—46 (2009).
154) For an example of catalytic asymmetric addition to ketones coupled with hydrogenation, see: Chmura A., van der Kraan G. M., van Langen L. M., van Rantwijk F., Sheldon R. A., *Adv. Synth. Catal.*, **348**, 1655—1661 (2006).
155) von Langermann J., Mell A., Paetzold E., Daußmann T., Kragl U., *Adv. Synth. Catal.*, **349**, 1418—1424 (2007).
156) Zuend S. J., Jacobsen E. N., *J. Am. Chem. Soc.*, **129**, 15872—15883 (2007).
157) Yazaki R., Kumagai N., Shibasaki M., *J. Am. Chem. Soc.*, **131**, 3195—3196 (2009).
158) For a comprehensive review of Lewis base catalysis, see: Denmark S. E., Beutner G. L., *Angew. Chem., Int. Ed.*, **47**, 1560—1638 (2008) and references cited therein.
159) For a selected example of Lewis base activation of a Brønsted base,

see: McGrath M. J., O'Brien P., *J. Am. Chem. Soc.*, **127**, 16378—16379 (2005).
160) For a selected example of Lewis base activation of a Brønsted base, see: Saito S., Tsubogo T., Kobayashi S., *J. Am. Chem. Soc.*, **129**, 5364—5365 (2007).
161) For a selected example of Lewis base activation of a Brønsted base, see: Morimoto H., Yoshino T., Yukawa T., Lu G., Matsunaga S., Shibasaki M., *Angew. Chem., Int. Ed.*, **47**, 9125—9129 (2008).
162) Enhanced Lewis basicity of LiOPh was observed by using bidentate phosphine oxide **25** in Mukaiyama aldol reactions. X-ray crystallographic analysis confirmed the coordination of **25** to Li cation in a bidentate fashion, Hatano M., Takagi E., Ishihara K., *Org. Lett.*, **9**, 4527—4530 (2007).
163) Yazaki R., Kumagai N., Shibasaki., *J. Am. Chem. Soc.*, **132**, 5522—5531 (2010).
164) Jagodzinski T. S., *Chem. Rev.*, **103**, 197—227 (2003) and references cited therein.
165) For an aldol reaction mediated by Grignard reagents, see: Tamaru Y., Harada T., Nishi S.-I., Mizutani M., Hioki T., Yoshida Z.-I., *J. Am. Chem. Soc.*, **102**, 7806—7808 (1980).
166) For a Michael reaction using *S*-silyl *N*,*S*-acetals, see: Goasdoue C., Goasdoue N., Gaudemar M., Mladenova M., *J. Organomet. Chem.*, **226**, 209—215 (1982).
167) For an aldol reaction using *S*-silyl *N*,*S*-acetals, see: Goasdoue C., Goasdoue N., Gaudemar M., *Tetrahedron Lett.*, **25**, 537—540 (1984).
168) For a Mannich reaction using *S*-silyl *N*,*S*-acetals, see: Goasdoue C., Gaudemar M., *Tetrahedron Lett.*, **26**, 1015—1018 (1985).
169) For an asymmetric aldol reaction mediated by a stoichiometric amount of a strong base and a chiral ligand, see: Iwasawa N., Yura T., Mukaiyama T., *Tetrahedron*, **45**, 1197—1207 (1989).
170) Suzuki Y., Yazaki R., Kumagai N., Shibasaki M., *Angew. Chem., Int. Ed.*, **48**, 5026—5029(2009).
171) "Comprehensive Organic Synthesis," Vol. 2, ed. by Trost B. M., Fleming I., Heathcock C.-H., Pergamon, Oxford, 1991.
172) For a comprehensive review, see ref. 111.
173) For a recent review of asymmetric aldol reactions, see: Palomo C., Oiarbide M., García J. M., *Chem. Soc. Rev.*, **33**, 65—75 (2004).
174) For a recent review of asymmetric aldol reactions, see: Geary L. M., Hultin P. G., *Tetrahedron: Asymmetry*, **20**, 131—173 (2009).
175) For a recent review of direct catalytic asymmetric aldol reactions, see refs. 111—118.
176) For a pioneering example of a direct catalytic asymmetric aldol reaction promoted by a metal-based catalyst, see: Yamada Y. M. A., Yoshikawa N., Sasai H., Shibasaki M., *Angew. Chem., Int. Ed.*, **36**, 1871—1873 (1997).
177) For an early example of a direct aldol-type reaction using α-isocyanoacetate as an active methylene type aldol donor, see: Ito Y., Sawamura M., Hayashi T., *J. Am. Chem. Soc.*, **108**, 6405—6406 (1986).
178) For a pioneering example of a direct catalytic asymmetric aldol reaction promoted by a metal-based catalyst, see: Yoshikawa N., Yamada Y. M. A., Das J., Sasai H., Shibasaki M., *J. Am. Chem. Soc.*, **121**, 4168—4178 (1999).
179) For a pioneering example of a direct catalytic asymmetric aldol reaction promoted by a metal-based catalyst, see: Trost B. M., Ito H., *J. Am. Chem. Soc.*, **122**, 12003—12004 (2000).
180) For a pioneering example of a direct catalytic asymmetric aldol reaction promoted by a metal-based catalyst, see: Mahrwald R., Ziemer B., *Tetrahedron Lett.*, **43**, 4459—4461 (2002).
181) For a pioneering example of a direct catalytic asymmetric intermolecular aldol reaction promoted by organocatalysts, see: List B., Lerner R. A., Barbas C. F. III, *J. Am. Chem. Soc.*, **122**, 2395—2396 (2000).
182) For a pioneering example of a direct catalytic asymmetric intermolecular aldol reaction promoted by organocatalysts, see: Sakthivel K., Notz W., Bui T., Barbas C. F. III, *J. Am. Chem. Soc.*, **123**, 5260—5267 (2001).
183) For a pioneering example of a direct catalytic asymmetric intermolecular aldol reaction promoted by organocatalysts, see: Saito S., Nakadai M., Yamamoto H., *Synlett*, **2001**, 1245—1248 (2001).
184) For direct catalytic asymmetric aldol (-type) reactions using aldol donors in the carboxylic acid oxidation state without electron-withdrawing α-substituents: alkylnitriles (up to 77% ee), see: Suto Y., Tsuji R., Kanai M., Shibasaki M., *Org. Lett.*, **7**, 3757—3760 (2005).
185) For direct catalytic asymmetric aldol (-type) reactions using aldol donors in the carboxylic acid oxidation state without electron-withdrawing α-substituents: activated amides (up to 33% ee), see: Saito S., Kobayashi S., *J. Am. Chem. Soc.*, **128**, 8704—8705 (2006).
186) For direct catalytic asymmetric aldol (-type) reactions using aldol donors in the carboxylic acid oxidation state without electron-withdrawing α-substituents: β,γ-unsaturated esters, see: Yamaguchi A., Matsunaga S., Shibasaki M., *J. Am. Chem. Soc.*, **131**, 10842—10843 (2009).
187) Iwata M., Yazaki R., Suzuki Y., Kumagai N., Shibasaki M., *J. Am. Chem. Soc.*, **131**, 18244—18245 (2009).
188) Iwata M., Yazaki R., Kumagai N., Shibasaki M., *Tetrahedron: Asymmetry*, **21**, 1688—1694 (2010).
189) Spletstoser J. T., White J. M., Tunoori A. R., Georg G. I., *J. Am. Chem. Soc.*, **129**, 3408—3419 (2007).
190) Robertson D. W., Jones N. D., Swartzendruber J. K., Yang K. S., Wong D. T., *J. Med. Chem.*, **31**, 185—189 (1988).
191) Robertson D. W., Krushinski J. H., Fuller R. W., Leander J. D., *J. Med. Chem.*, **31**, 1412—1417 (1988).
192) Henry M. E., Schmidt M. E., Hennen J., Villafuerte R. A., Butman M. L., Tran P., Kerner L. T., Cohen B., Renshaw P. F., *Neuropsycopharmacology*, **30**, 1576—1583 (2005) and references cited therein.
193) Sundberg R. J., Walters C. P., Bloom J. D., *J. Org. Chem.*, **46**, 3730—3732 (1981).
194) Srebnik M., Ramachandran P. V., Brown H. C., *J. Org. Chem.*, **53**, 2916—2920 (1988).
195) Li Y., Li Z., Li F., Wang Q., Tao F., *Org. Biomol. Chem.*, **3**, 2513—2518 (2005) and references cited therein.
196) Garro-Helion F., Merzouk A., Guibé F., *J. Org. Chem.*, **58**, 6109—6113 (1993).